

Tectono-stratigraphic evolution and crustal architecture of the Orphan Basin during North Atlantic rifting

Mohamed Gouiza¹ · Jeremy Hall² · J. Kim Welford²

Received: 1 February 2016 / Accepted: 25 May 2016 / Published online: 3 June 2016
© The Author(s) 2016. This article is published with open access at Springerlink.com

Abstract The Orphan Basin is located in the deep offshore of the Newfoundland margin, and it is bounded by the continental shelf to the west, the Grand Banks to the south, and the continental blocks of Orphan Knoll and Flemish Cap to the east. The Orphan Basin formed in Mesozoic time during the opening of the North Atlantic Ocean between eastern Canada and western Iberia–Europe. This work, based on well data and regional seismic reflection profiles across the basin, indicates that the continental crust was affected by several extensional episodes between the Jurassic and the Early Cretaceous, separated by events of uplift and erosion. The preserved tectono-stratigraphic sequences in the basin reveal that deformation initiated in the eastern part of the Orphan Basin in the Jurassic and spread towards the west in the Early Cretaceous, resulting in numerous rift structures filled with a Jurassic–Lower Cretaceous syn-rift succession and overlain by thick Upper Cretaceous to Cenozoic post-rift sediments. The seismic data show an extremely thinned crust (4–16 km thick) underneath the eastern and western parts of the Orphan Basin, forming two sub-basins separated by a wide structural high with a relatively thick crust (17 km thick). Quantifying the crustal architecture in the basin highlights the large discrepancy between brittle extension localized in the upper crust and the overall crustal thinning. This suggests that continental deformation in the Orphan Basin involved, in addition to the documented Jurassic and Early Cretaceous rifting, an

earlier brittle rift phase which is unidentifiable in seismic data and a depth-dependent thinning of the crust driven by localized lower crust ductile flow.

Keywords Passive margins · Rift basins · Tectonics · Sedimentation

Introduction

The opening of the North Atlantic Ocean between eastern Newfoundland and western Iberia–Europe started with continental rifting in the Late Triassic to Early Jurassic which led to continental break-up and the initiation of ocean crust in the Aptian–Albian (e.g. Welsink et al. 1989; Grant and McAlpine 1990; Bassi et al. 1993; Enachescu et al. 2005; Tucholke et al. 2007; Alves et al. 2009). Continental rifting was initially driven by an early NW–SE crustal extension between SW Newfoundland and Iberia in the Late Triassic–Early Jurassic and then propagated northward between NW Newfoundland and western Europe in the Middle Jurassic–Early Cretaceous (Fig. 1) (Tankard and Welsink 1989; Enachescu et al. 2005). Around the Aptian–Albian, continental break-up took place between Newfoundland and Iberia–Europe and involved major geodynamic changes in the evolution of the North Atlantic, as it led to the separation of the Grand Banks from Iberia, and the Flemish Cap from the Galicia Bank (Williams 1984; Tucholke et al. 2007). In the Late Cretaceous, extension propagated further north and initiated the opening of the Labrador Sea between Labrador and West Greenland (Chian et al. 1995; Chalmers et al. 1999; Enachescu 2006; Dickie et al. 2011).

The Late Triassic–Early Cretaceous crustal extension resulted in several major rift basins like the Porcupine, Rockall, and Hatton basins off the Irish margin (Fig. 1) and

✉ Mohamed Gouiza
m.gouiza@leeds.ac.uk

¹ School of Earth and Environment, University of Leeds, Leeds LS2 9JT, England, UK

² Department of Earth Sciences, Memorial University of Newfoundland, St. John's, Canada

Fig. 1 Reconstruction of the central North Atlantic to Chron M0 (ca. 125 Ma) (modified from Tucholke and Sibuet 2012; Pe-Piper et al. 2013) showing the distribution of the major Early Cretaceous basins according to Welford et al. (2010)

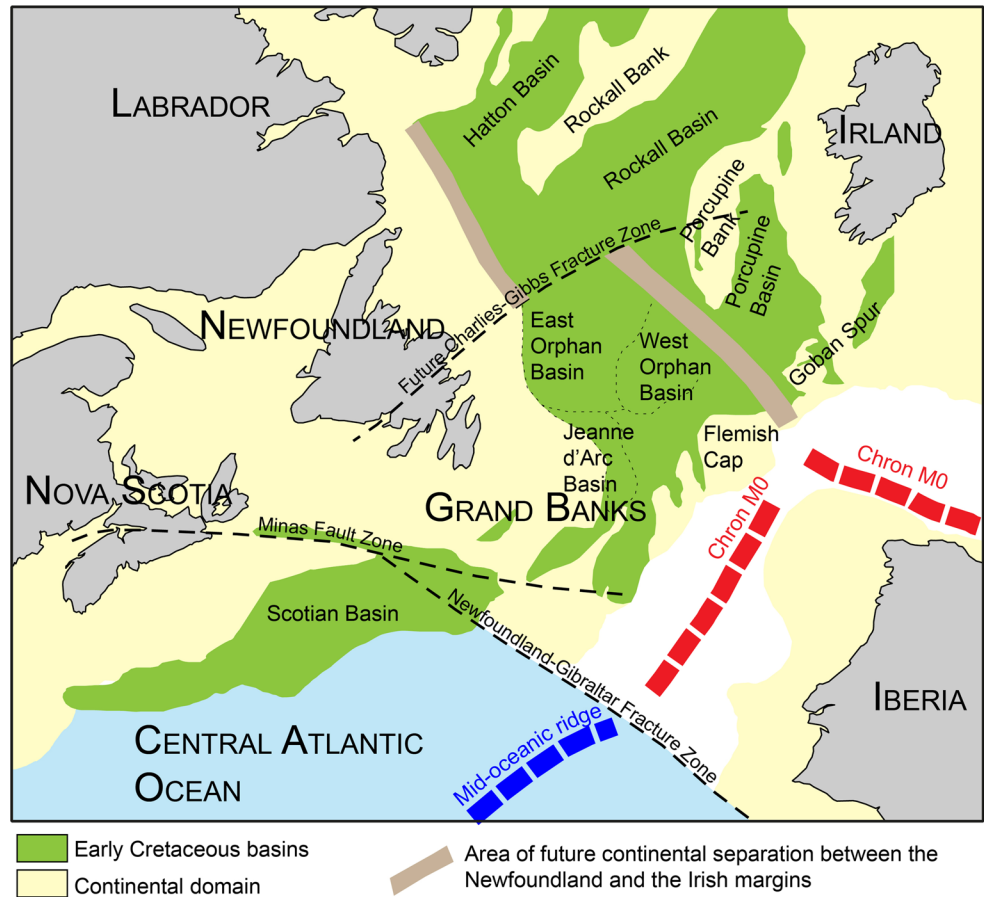
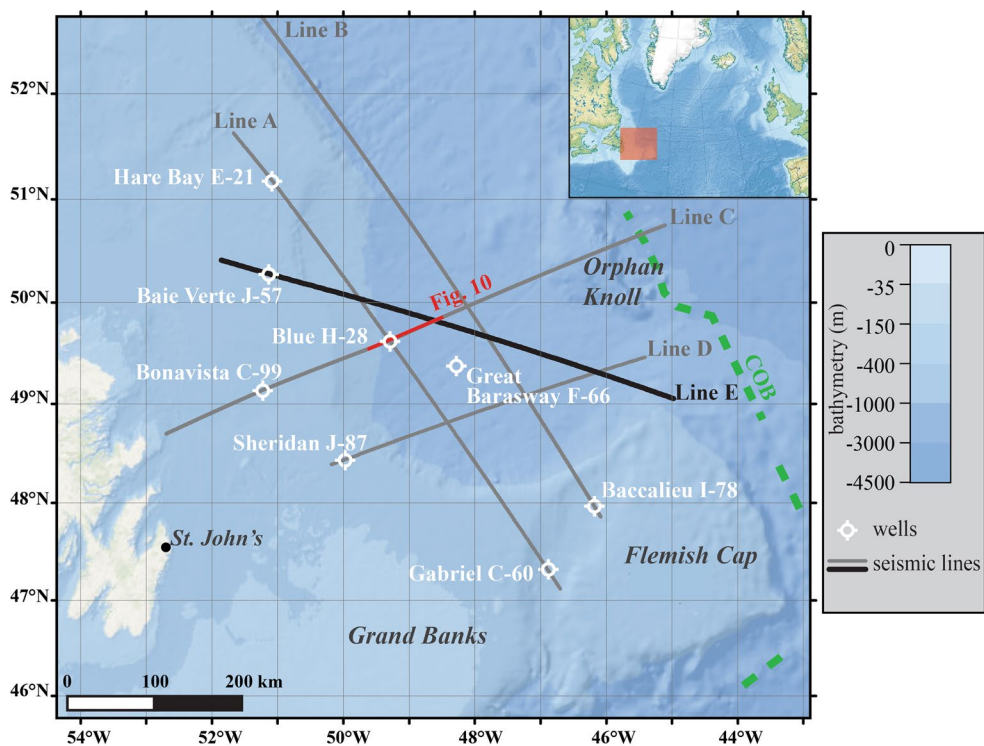


Fig. 2 Bathymetric map of the Orphan Basin showing the seismic reflection profiles, plotted with solid lines, and the well data, plotted with white circles, considered in this work. A portion of the seismic profile C, highlighted in red, is displayed in detail in Fig. 11. Seismic line E is shown entirely and in detail in Figs. 6, 10, and 12. Seismic data courtesy of TGS. COB: interpreted continent–ocean boundary according to Funck et al. (2003)



the Orphan Basin off the Newfoundland margin (Fig. 2) (Vogt et al. 1998; Mackenzie et al. 2002; Enachescu 2006; O'Reilly et al. 2006; Yang 2012; Dafoe et al. 2015; Lau et al. 2015). The Orphan Basin, which is the focus of this study, is a deep-water rift basin surrounded by the Newfoundland continental shelf in the west, the Grand Banks in the south, the Flemish Cap in the southeast, and the Orphan Knoll in the northeast (Fig. 2). Geophysical data from the basin show a highly thinned crust and a thick Mesozoic–Cenozoic sedimentary cover (e.g. Chian et al. 2001; Welford and Hall 2007; Lau et al. 2015). The East Orphan Basin appears to be older as it contains Jurassic syn-rift sediments, while the West Orphan Basin is younger as the first syn-rift sediments are assumed to be Lower Cretaceous (Enachescu et al. 2004, 2005). Despite the strong crustal thinning that is observed underneath the East and West Orphan depocentres, the Aptian–Albian continental break-up between the Newfoundland and the Irish margins occurred immediately east of the Orphan Knoll and the Flemish Cap (Figs. 1, 2) (Funck et al. 2003; Welford et al. 2012).

Although several contributions have examined the large-scale structural and crustal architecture of the Orphan Basin (e.g. Enachescu et al. 2004, 2005; Welford et al. 2012; Watremez et al. 2015; Lau et al. 2015), only few tried to quantify its Mesozoic syn-rift history and the driving tectonic processes (Dafoe et al. 2015; Gouiza et al. 2015). In this contribution, (1) we examine the stratigraphic and tectonic evolution of the Orphan Basin using exploration wells and regional seismic lines, (2) we investigate its structural and crustal architectures to quantify amounts of crustal extension versus crustal thinning during rifting, and (3) we propose tectonic processes that can explain its tectono-stratigraphic evolution.

Data and methods

Well data

Several exploration wells, drilled offshore of the Newfoundland margin, are used in this work to characterize the Mesozoic sediments across the Orphan Basin (Figs. 2, 3). Four wells are located on the continental shelf (Hare Bay E-21, Baie Verte J-57, Bonavista C-99, and Sheridan J-87), two wells are found in the deep basin (Blue H-28 and Great Barasway F-66), and two wells in the Flemish Pass (Baccalieu I-78 and Gabriel C-60) (Figs. 2, 3). Other than the Great Barasway F-66 which was drilled on a roll-over structure (Gacal-Isler 2009), the wells in the Orphan Basin were drilled on structural highs characterized by a very reduced Mesozoic succession and, mostly, no syn-rift sediments (Fig. 3). We use the wells from the Flemish Pass

Basin, which exhibit thicker Mesozoic series, to draw correlations into the deeper parts of the Orphan Basin.

2D seismic reflection data

Five deep marine multichannel seismic reflection lines (labelled A to E; Fig. 2) were acquired by TGS in the Orphan Basin in 2002. Lines A and B extend NW–SE over 617.9 and 677.54 km, respectively. Lines C and D run NE–SW over 593.07 and 369.36 km, respectively. Line E is oriented WNW–ESE and is 518.75 km long. All lines were recorded to a maximum two-way time (TWT) of 12 s and were provided to us (courtesy of TGS) in time-migrated SEG-Y format.

In this study, we focus on seismic line E, which was interpreted initially in the time domain and then converted to depth. We used the unconformities identified in the wells (Figs. 3, 4, 5) as regional markers to correlate the lithostratigraphic successions along the seismic lines. Five seismo-stratigraphic units were identified, namely the Cenozoic, the Upper Cretaceous, the Lower Cretaceous, the Jurassic, and the pre-Mesozoic basement (Figs. 5, 6). After stratigraphic interpretation was accomplished by picking the different horizons in the time domain, seismic line E was depth-converted using interval velocities. Stacking velocities along the profile (Fig. 7), provided by TGS, were converted to interval velocities using the Dix formula (Dix 1955) and then used to infer an interval velocity function for each seismo-lithological unit (Fig. 8).

$$V_{\text{int}} = \left[\left(t_2 V_{\text{RMS2}}^2 - t_1 V_{\text{RMS1}}^2 \right) / (t_2 - t_1) \right]^{1/2} \quad (\text{Dix formula})$$

where V_{int} is interval velocity; t_1 is travelttime to the first reflector; t_2 is travelttime to the second reflector; V_{RMS1} is root-mean-square velocity to the first reflector; and V_{RMS2} is root-mean-square velocity to the second reflector.

Uncertainties related to the time-to-depth conversion produce minor thickness errors, of no consequence to this analysis, in the depth-converted lines when calibrated with the wells (Fig. 9).

Mesozoic sedimentary architecture in the Orphan Basin from well and 2D seismic reflection data

Seismo-stratigraphic units

Well data from the Orphan Basin, when correlated with the seismic reflection profiles, reveal the existence of four stratigraphic unconformities in the syn-rift and early post-rift sequences (Fig. 3). These are the Tithonian unconformity, the Aptian–Albian unconformity, the Santonian

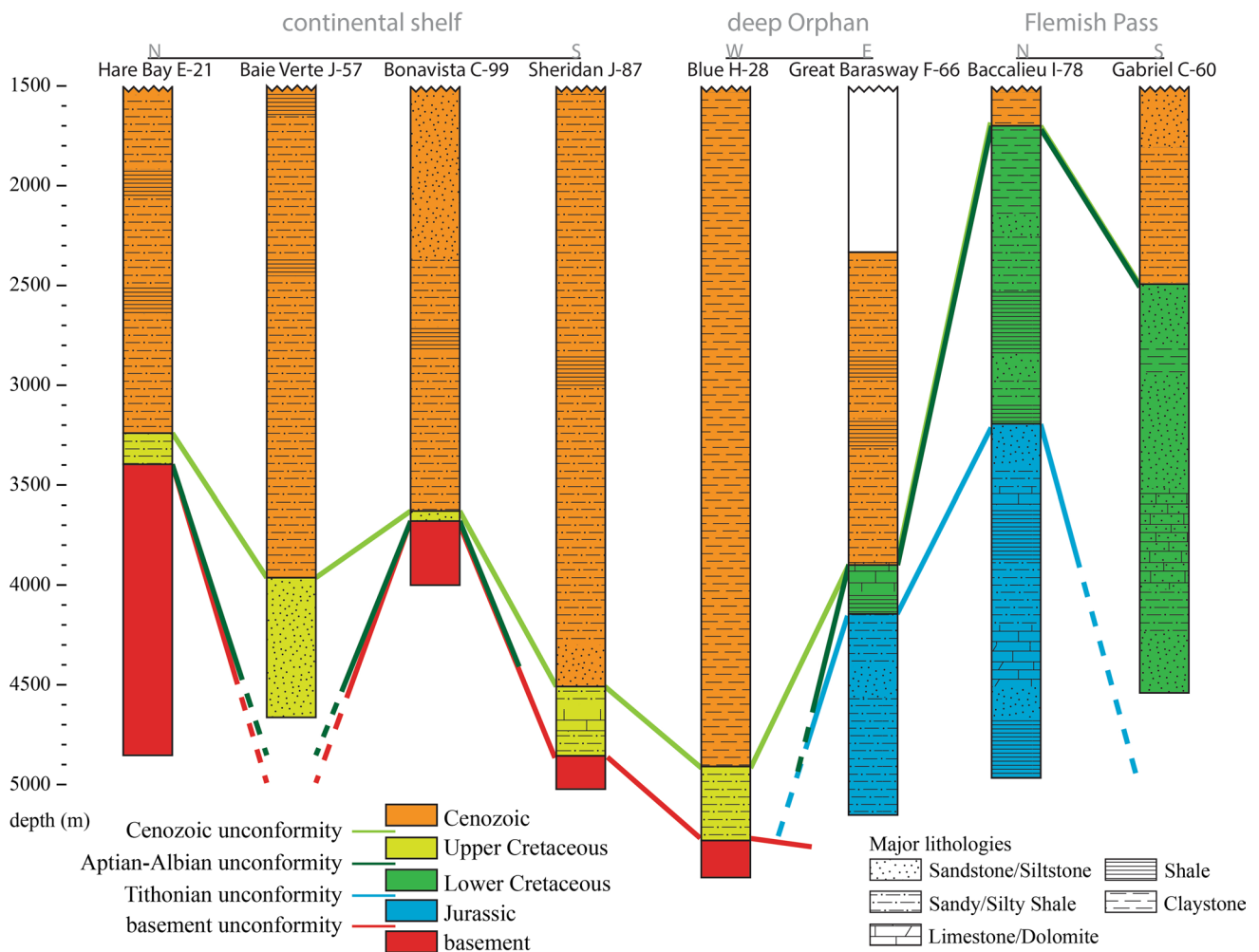


Fig. 3 Simplified stratigraphic logs of the exploration wells found in the Orphan Basin and used in this work. They show the main lithologies and the major stratigraphic unconformities correlated across the basin

unconformity, and the base Cenozoic unconformity (Enachescu et al. 2005; Dafoe et al. 2015). Most of these unconformities form prominent seismic horizons that were picked and correlated as regional markers along the seismic profiles, except the Santonian unconformity which was only identified in the Baie Verte J-57 well. According to Dafoe et al. (2015), the Santonian unconformity is only recognized in proximal parts of the West Orphan Basin wells (e.g. Baie Verte J-57) and appears to change to paraconformity in the East Orphan Basin. Therefore, five major seismo-stratigraphic units were identified in the Orphan Basin defined by the major depositional and erosional unconformities and distinct seismic facies (Figs. 5, 6, 9):

- The Cenozoic succession, characterized in the well logs by the Cenozoic unconformity at its base, is extremely thick on the continental shelf (3000–4000 m), but thins towards the east in the deep basin (1500 m) and towards

the southeast in the Flemish Pass (600–1400 m). The Cenozoic succession is formed by the Banquereau Formation and consists mainly of shales, mudstones, and thin intercalations of carbonates. On seismic data, this unit is characterized by continuous high-amplitude reflections alternating with very weak amplitude reflections (Figs. 5, 6).

- The Upper Cretaceous succession is defined by the Cenozoic unconformity at the top and the Aptian–Albian unconformity at the base. The latter unconformity was initially interpreted as base Cenomanian (Enachescu et al. 2005), but new palynological analyses yielded a more reliable age at the Aptian–Albian boundary (Dafoe et al. 2015). The Upper Cretaceous succession is drilled in the continental shelf (650 m thick in Baie Verte J-57) and the deep Orphan Basin where it becomes significantly thin towards the east (10 m thick in Great Barasway F-66). It mainly consists of the

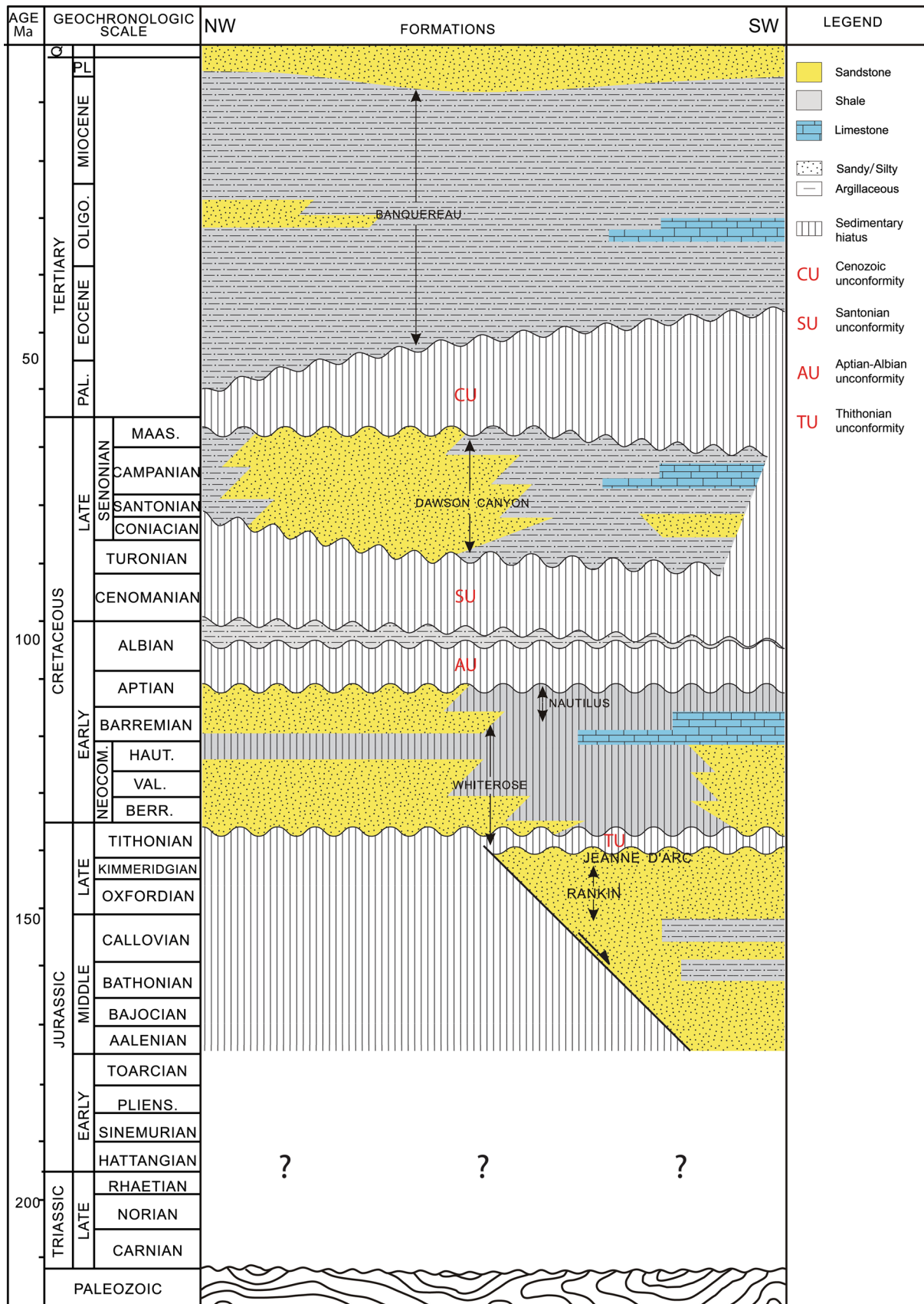


Fig. 4 Simplified lithostratigraphic chart of Orphan Basin based on available exploration wells (Figs. 2, 3)

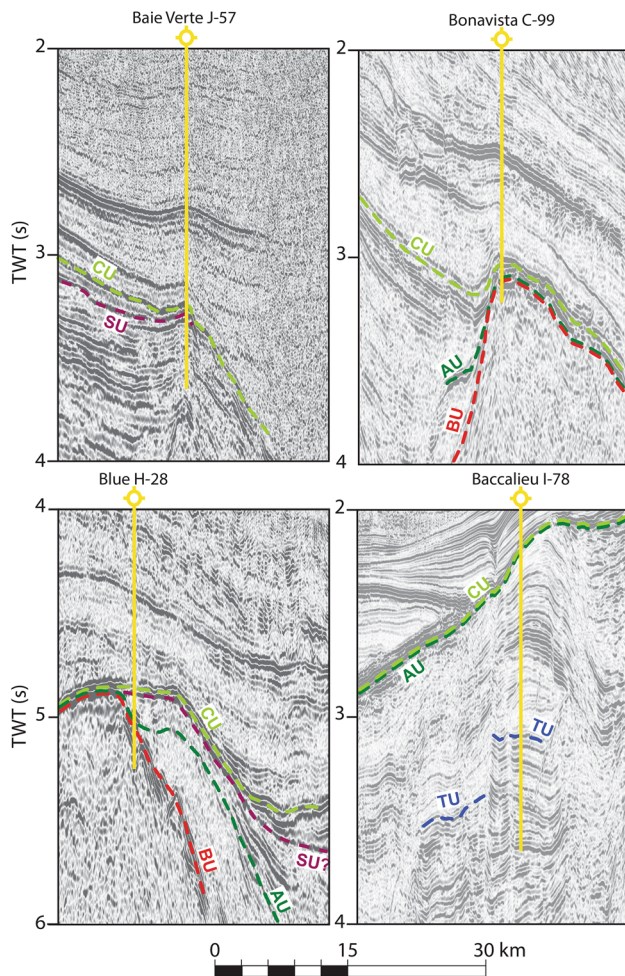


Fig. 5 The Baie Vert J-57, Bonavista C-99, Blue H-28, and Baccalieu I-78 wells tied and calibrated with the seismic data in time domain. Light green, purple, dark green, blue, and red horizons represent the base Cenozoic unconformity (CU), the Santonian unconformity (SU), the Aptian–Albian unconformity (AU), the Tithonian unconformity (TU), and the Basement top (BU), respectively. Location of well and seismic data is shown in Fig. 2. Seismic data courtesy of TGS

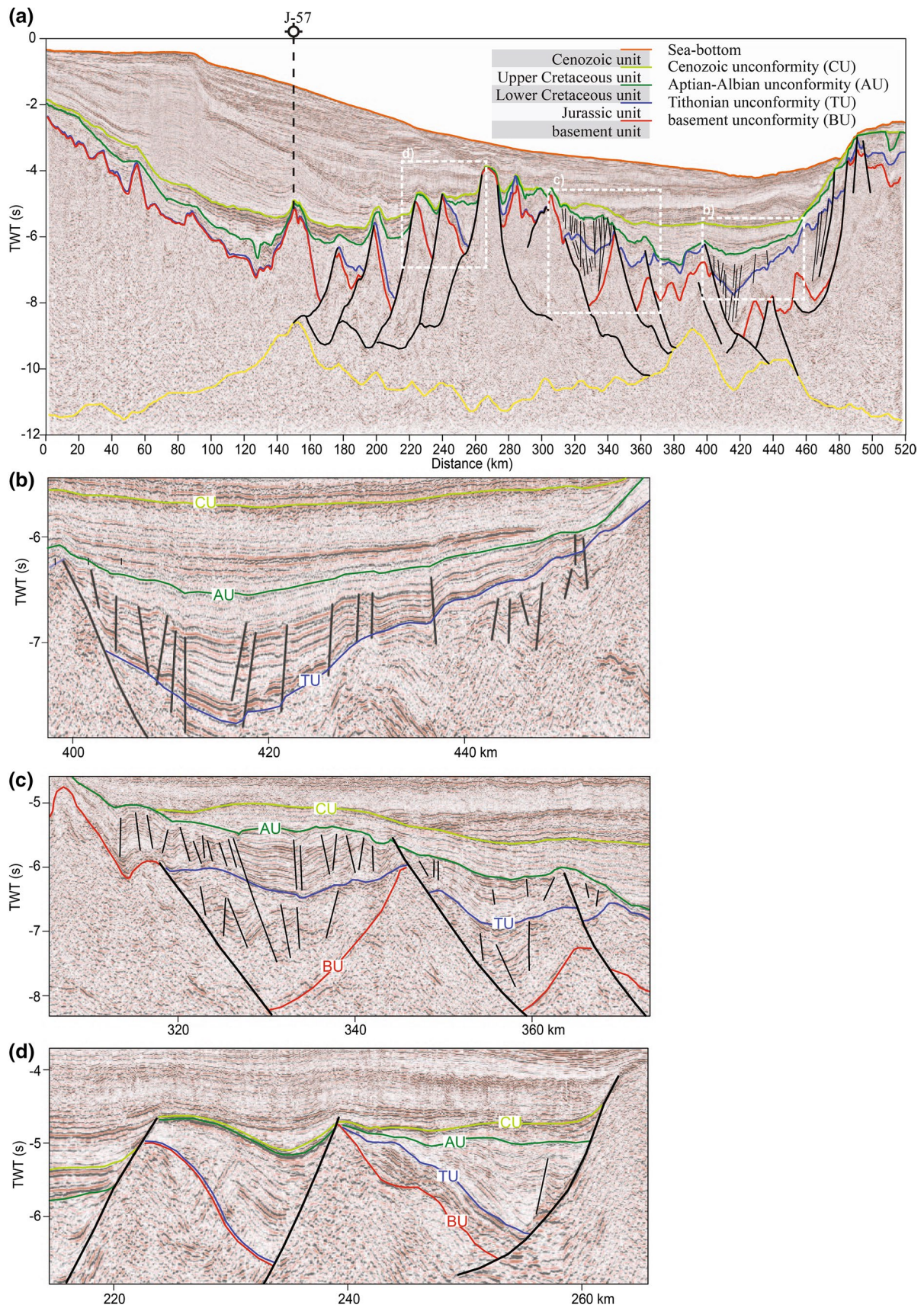
Cenomanian–Campanian Dawson Canyon Formation and contains predominantly medium- to coarse-grained siliciclastic sediments (siltstones and sandstones), mudstones, and marls in the south (Sheridan J-87). The Upper Cretaceous unit shows two different seismic signatures on seismic profiles. It is mainly characterized by continuous low-amplitude and low-frequency reflections in the eastern part of the basin and overlain by continuous high-amplitude and high-frequency reflections in the western part of the basin (Figs. 5, 6). This sequence roughly corresponds to the breakup sequence recognized in Northwest Iberia by Soares et al. (2012).

- The Lower Cretaceous succession is defined by an Aptian–Albian unconformity at the top and the Titho-

Fig. 6 a Interpreted seismic line E in the time domain illustrating the stratigraphic and structural architecture of the Orphan Basin. Interpretation of the Moho discontinuity is plotted with a solid yellow line. b–d Illustrating in more detail the relationship between the different seismo-stratigraphic units and their distribution within the half-graben structures

nian unconformity at the base. It is found only in the East Orphan Basin (Great Barasway F-66) and the Flemish Pass wells (Baccalieu I-78 and Gabriel C-60). It includes mainly the Nautilus Formation and the Whitrose Formation, formed by shale-dominated series with occasional siltstone and sandstone interbeds. This unit has a recognizable seismic signature along the profiles consisting of discontinuous reflections with medium to low amplitudes and high to medium frequencies (Figs. 5, 6).

- The Jurassic succession, capped by the Tithonian unconformity, occurs only in the Great Barasway F-66 and the Baccalieu I-78 wells in the East Orphan Basin and Flemish Pass, respectively. It includes the Tithonian Jeanne d’Arc Formation and the Callovian–Kimmeridgian Rankin Formation, which consist of shales, siltstones, sandstones, and minor limestone interbeds. The base of this succession was never drilled in this area, and the age of the first Mesozoic sediments deposited in the Orphan Basin, in relation to the Atlantic rifting, has yet to be determined. However, well data in the Jeanne d’Arc Basin to the south indicate the presence of Upper Triassic clastics lying unconformably over the Palaeozoic basement (McAlpine 1990). This configuration is similar to West Iberia (Alves et al. 2003), West France (Roberts and Bally 2012), and West Ireland (Murphy and Ainsworth 1991). In this work, the Jurassic succession includes the sediments between the Tithonian unconformity and the Palaeozoic basement, which may or may not include Upper Triassic deposits. The Jurassic unit is very thin and scattered in the western part of the basin where it is represented by discontinuous high-amplitude reflections. It is much thicker in the eastern part of the basin and characterized by medium- to very-low-amplitude reflections (Figs. 5, 6). The major uncertainty in our seismic interpretation is the Jurassic deposits drilled only in the East Orphan Basin and for which there is no direct evidence in the west.
- The oldest succession, encountered in wells drilled on structural highs, is the pre-Mesozoic basement probably of Palaeozoic to Neoproterozoic age. It comprises low-grade metamorphosed sediments and igneous granitic rocks. The basement is characterized in seismic data by chaotic and discontinuous reflections with medium to high amplitudes (Figs. 5, 6).



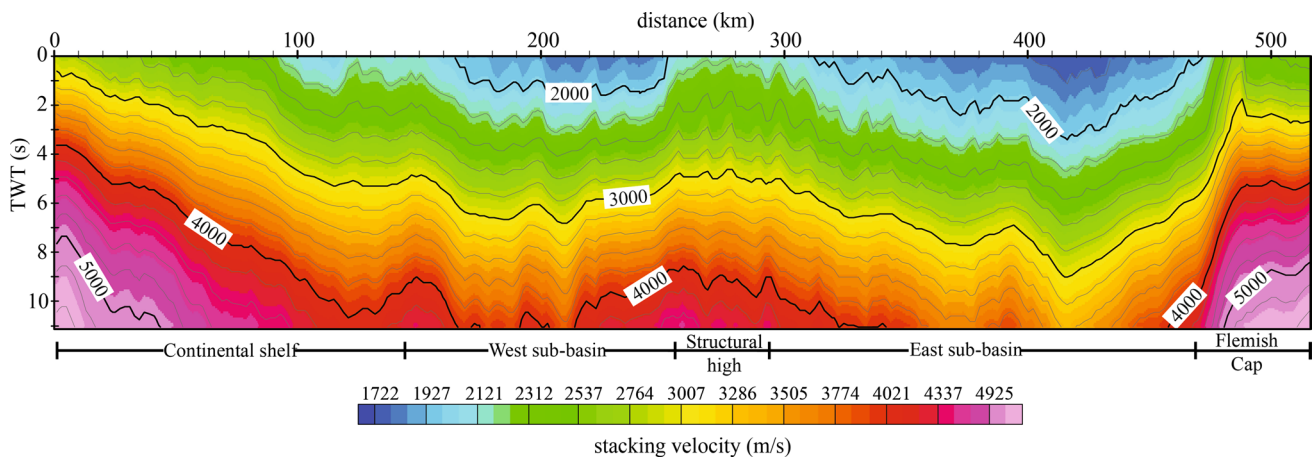


Fig. 7 Grid showing variation of stacking velocity with time (TWT) along seismic line E. Stacking velocity data courtesy of TGS

Structural and stratigraphic architecture imaged by the 2D seismic data

Seismic line E (Figs. 6, 10) reveals that rifting and crustal stretching in the Orphan Basin resulted in two extensional systems separated by a horst structure. In the East Orphan sub-basin, extension was accommodated by wide half-graben bounded mainly by east-dipping listric normal faults (Figs. 6, 10). In the West Orphan sub-basin, extension occurred along steeper normal faults that dip towards the west and define narrower half-graben and eastward tilted blocks with pronounced ridges (Figs. 6, 10, 11). The sedimentary infill of the extensional structures is primarily composed of Jurassic and Lower Cretaceous successions.

The Jurassic sediments are found mainly in the eastern domain of the basin to the east of the horst structure, where they show large thickness variations related to east-dipping normal faults. They show growth strata and thickening towards the faults (Fig. 6a–c), a character indicating a syn-tectonic deposition during crustal stretching. The Jurassic deposits get much thinner and scattered as we move to the west of the horst structure, and are absent on the continental shelf. They are characterized by sub-parallel reflections with no evidence of syn-depositional tectonics in the western part of the Orphan Basin (Figs. 6a, d, 11). The Jurassic succession is capped by an erosional unconformity (Tithonian unconformity) across the basin illustrated on the seismic data by truncated reflections (Fig. 6).

The Lower Cretaceous sediments unconformably overlay the Jurassic and show more lateral continuity across the deep basin and the continental shelf (Figs. 6, 10). Their thickness is relatively constant across the continental shelf, but shows substantial variations in the deeper domains of the basin where the normal faulting appears to have controlled sedimentation. This is particularly the case in the western part of the deep basin where the Lower Cretaceous

package is characterized by significant thickening inside the half-graben and strata growth patterns towards the faults (Figs. 6d, 11), a character yet again similar to West Iberia's Lusitanian Basin (Alves et al. 2003, 2006, 2009) and offshore Ireland (Shannon et al. 2001). East of the horst structure, the Lower Cretaceous succession is also affected by syn-rift normal faults but displays smaller offsets than in the west. The topmost seismic reflections of this sedimentary unit exhibit truncation patterns related to the Aptian–Albian erosional unconformity (Figs. 6, 10).

The Upper Cretaceous succession seals most of the syn-rift structures in the eastern part of the basin (Figs. 6b, c, 10), where it is characterized by sub-parallel reflections onlapping the underlying Aptian–Albian unconformity. It is much thinner in the western part of the basin (Figs. 6d, 11) between the continental shelf and the horst structure where the west-dipping faults were still active and the tilted block ridges remained emerged during Late Cretaceous time.

The Cenozoic succession has a very consistent character across the entire Orphan Basin. Its base shows reflections sub-parallel to the underlying Upper Cretaceous with no evidence of erosional or angular unconformity. This succession is extremely thick above the edge of the continental shelf and thins considerably as we move to the east of the basin (Figs. 6, 10). Its internal architecture is well imaged along the different seismic profiles but will not be discussed in detail in this work as the main focus is on the syn-rift evolution.

Crustal structure of the Orphan Basin

Moho and crustal thickness along seismic line E

Our Moho interpretation corresponds to the base of high-amplitude reflections located in the deeper part of the

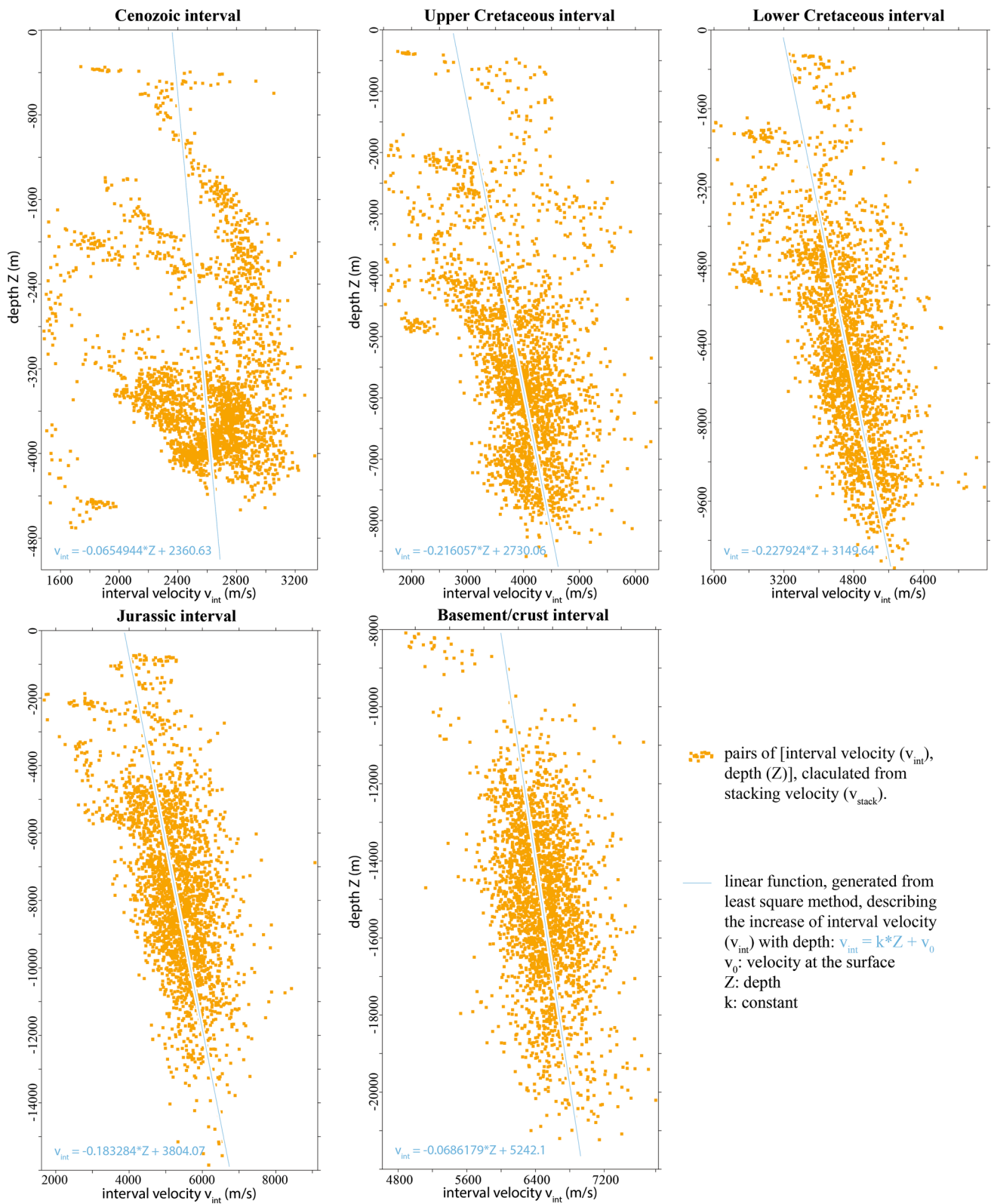
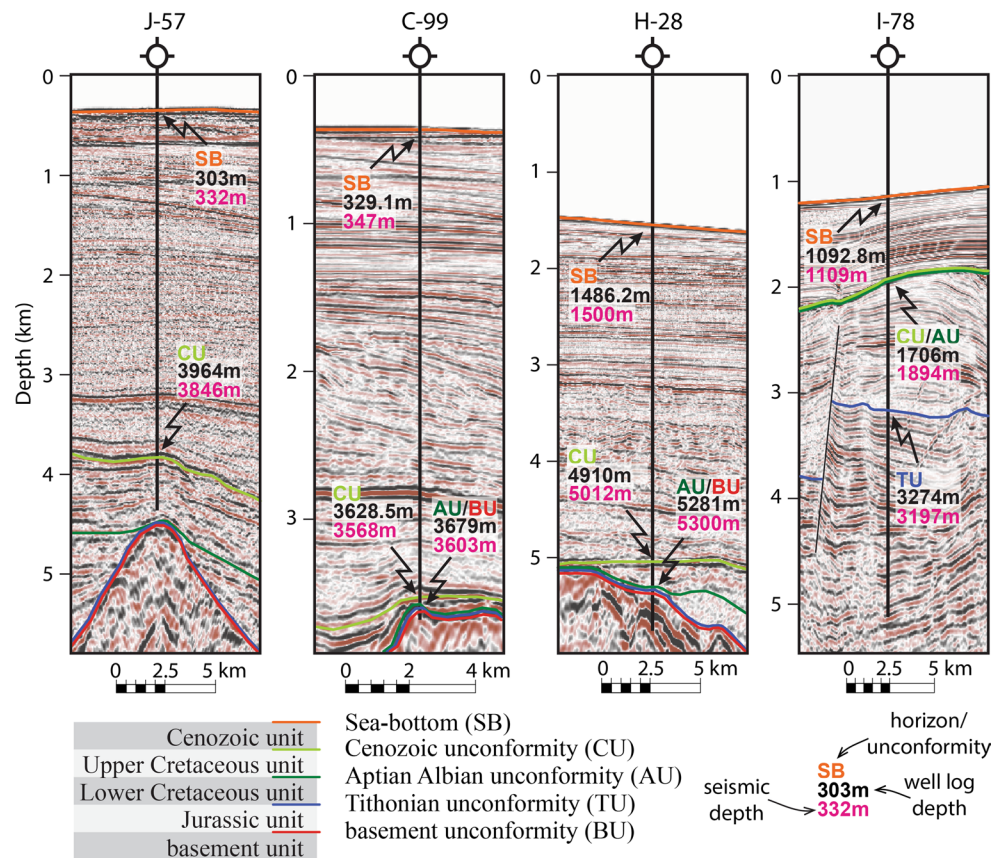


Fig. 8 Cross-plots of [interval velocity, depth] pairs for each seismo-lithostratigraphic unit calculated from stacking velocities (Fig. 7) using the Dix formula (Dix 1955)

Fig. 9 Four seismic–well ties in the depth domain showing the correlation between the lithological unconformities from the well logs (in black) and the depth of the interpreted seismic horizons (in pink) (seismic data courtesy of TGS). J-57: Baie Verte well; C-99: Bonavista well; H-28: Blue well; I-78: Baccalieu well



seismic section, below moderately reflective layering above and lower reflectivity below (Fig. 12). These reflections are shallow and continuous underneath the faulted crystalline basement, but become diffuse and discontinuous as they deepen below the rigid crustal blocks (Fig. 12). While the Moho ‘pick’ is somewhat uncertain in the seismic reflection imaging, there is generally a reasonable correlation with wide-angle seismic results and gravity modelling (see below). Furthermore, the crustal seismic velocities used for the depth conversion range between 5790 m/s in the shallowest part of the crust and 6750 m/s in deepest part of the crust (Fig. 8). This is consistent with crustal velocity estimates from wide-angle seismic data in the basin (Watremez et al. 2015; Lau et al. 2015).

The crustal architecture of the Orphan Basin, illustrated on seismic line E (Fig. 12) crossing the Orphan Basin in a WNW–ESE direction, clearly shows the existence of four distinct crustal domains. The continental shelf domain to the west is characterized by the thickest post-rift succession (up to 7000 m), a very thin syn-rift (<2000 m), and no syn-rift faulting affecting the basement. The crust is 28 km thick in the west where the Moho is 30 km deep, but thins progressively and considerably towards the east where the Moho is 15 km deep and the crust is only 7 km thick. The western sub-basin domain displays a thick post-rift

succession in the west (<5500 m), which is much thinner in the east (<2500 m), and isolated syn-rift depocentres in the half-graben filled mainly by Lower Cretaceous sediments (<3000 m thick). The crust is affected by a series of west-dipping faults, which bound the half-graben and sole out at a mid-crustal detachment ~14 to 15 km deep (Fig. 12). The crust is 9 km thick in the west and 16 km thick in the east. The crust thickens as the Moho deepens towards the east but thins locally under the half-graben where it may be only 5 km thick. The eastern sub-basin domain is separated from the western sub-basin by a 150-km-wide structural high, showing very reduced syn- and post-rift successions (<3000 m thick) and a 17-km-thick crust with a 21- to 22-km-deep Moho. The eastern sub-basin is covered by a 2.5- to 4-km-thick post-rift succession, overlying the Jurassic–Lower Cretaceous syn-rift sediments (<5000 m thick), which fill the half-graben. This domain is affected by major east-dipping listric normal faults soling out at the Moho level. The crust is 12 to 15 km thick in the west but only 4 km thick in the east. The Moho underneath the sub-basin shallows rapidly towards the east, reaches a minimum depth of 12 km in the centre, and remains about 14 km deep in the east (Fig. 12).

Figure 13 displays a comparison between our interpretation of the basement top and the Moho along seismic line

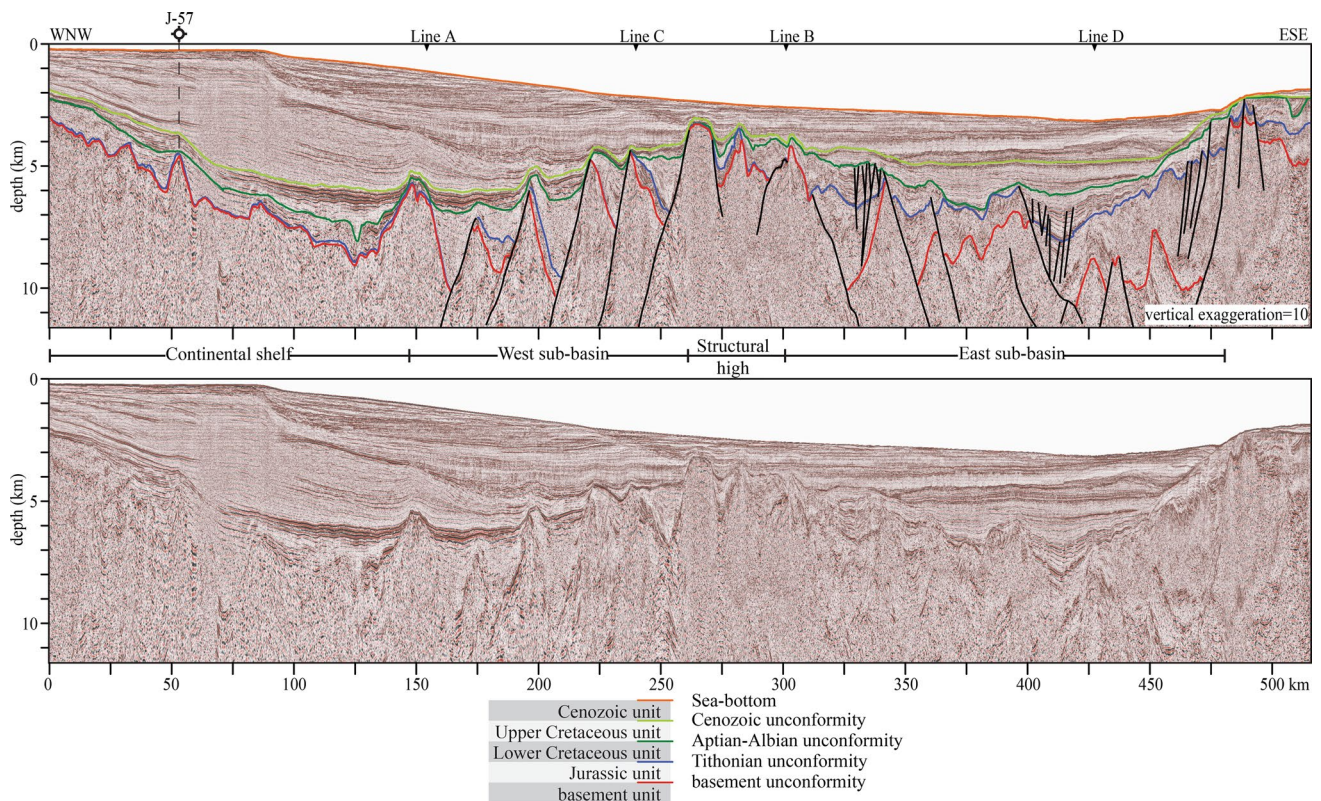


Fig. 10 Upper crustal portion of the depth-converted seismic line E. The *upper panel* shows the stratigraphic and structural interpretation of the seismic reflection data. The *lower panel* displays the seismic data without interpretation (seismic data courtesy of TGS)

E with the basement top and Moho predicted by Welford et al. (2012) in their 3D gravity inversions. Although the first-order variations in the basement topography compare favourably, it is 1 to 2 km deeper in the continental shelf domain and 2 to 3 km shallower in the eastern sub-basin, especially underneath the half-grabens. However, the Moho topography predicted from the gravity data is smoother and varies between 22 and 15 km depth, while the seismic data suggest a Moho ranging between 30 and 12 km depth with more abrupt changes, notably beneath the continental shelf and the eastern part of the basin. The mismatches are likely due to the basement depth constraints, the lower-frequency content of the satellite gravity data, and the density bounds used in the inversion (Welford et al. 2012).

Recent results from traveltimes tomography and dense wide-angle reflection data along the OBWAVE line (Lau et al. 2015; Watremez et al. 2015), which is slightly oblique to our seismic line E (Fig. 14a), show a crustal structure comparable to our interpretation. They demonstrate the existence of two sub-basins with extremely thinned crust (<10 km) and separated by a narrow domain (80 km wide) with a 20-km-thick crust. Nevertheless, they estimate a much thicker crust underneath the Flemish Cap (32 km thick) and a much steeper Moho shallowing at the

transition between the continental shelf and the western Orphan sub-basin.

2D gravity model along Line E

We performed 2D forward gravity modelling along line E, using the GM-SYS profile modelling module in Geosoft Oasis Montaj software, to assess the consistency of our interpretation of the Moho and the resulting crustal structure (Fig. 14). We use the satellite altimetry gravity anomalies (Fig. 14a) (Sandwell and Smith 2009), which can be downloaded from Scripps Institution of Oceanography (<https://scripps.ucsd.edu/>). The free-air gravity anomalies in the Orphan Basin are overall negative and surrounded by strong gravity highs over the continental shelf, the Flemish Cap, and the Orphan Knoll (Fig. 14a). A narrow N–S elongated gravity high is also shown within the Orphan Basin and corresponds to the structural high domain, which is documented along the seismic lines between the eastern and western sub-basins.

The depth-converted seismic line E was simplified for gravity modelling purposes. It was subdivided into six sub-horizontal layers: sea water, post-rift sediments, syn-rift sediments, upper crust, lower crust, and upper mantle, and

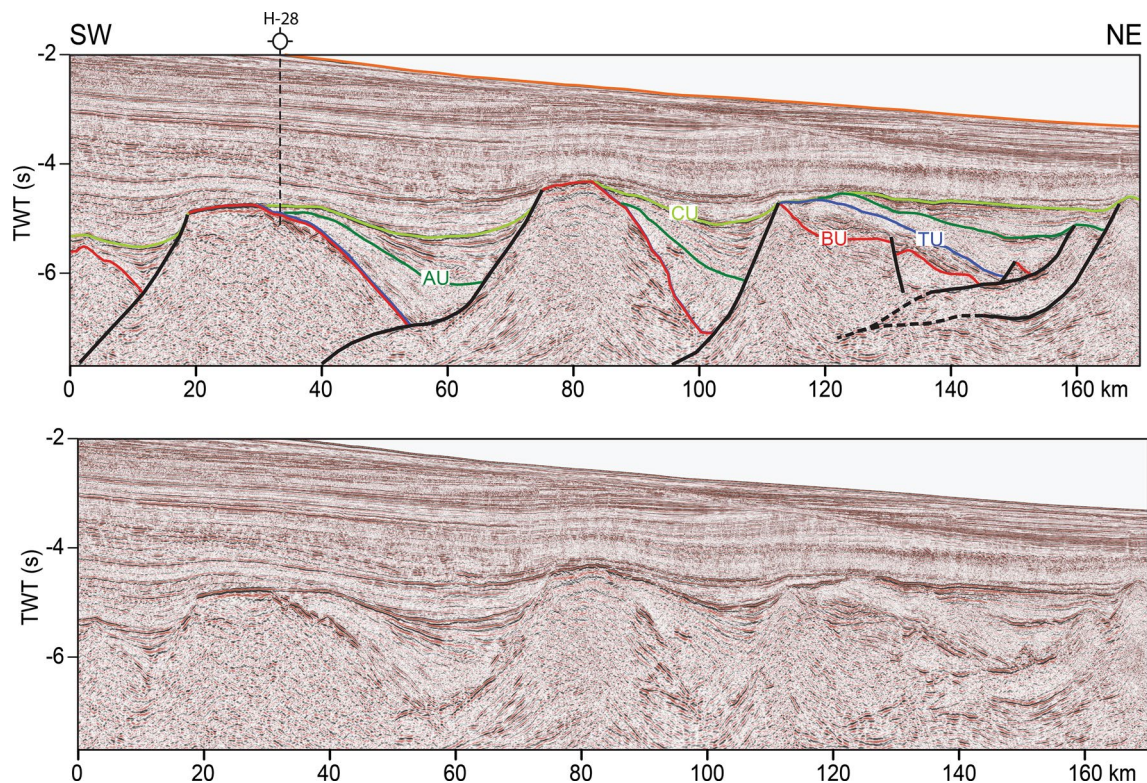


Fig. 11 Portion of the seismic reflection profile C in the time domain showing extensional systems defined by west-dipping normal faults, characteristic of the Early Cretaceous rifting phase localized in the

West Orphan Basin (seismic data courtesy of TGS). Faults are plotted with *solid black lines*. Colours of the stratigraphic horizons are described in the caption of Fig. 5. Location is shown in Fig. 2

each layer was given an average initial density based on the density analysis shown in Fig. 15. The latter figure illustrates density variation along line E derived from interval velocities using Gardner's equation, which describes the relationship between P-wave velocity and density (Gardner et al. 1974). It shows that density ranges between 2100 and 2600 kg/m³ in syn- and post-rift sediments, 2400–2700 kg/m³ in the upper crust, and 2700–2900 kg/m³ in the lower crust. The forward modelling was constrained by fixing the thickness of the sedimentary layers and the crust, and the density of the sea water. The densities of the other layers and the mid-crustal boundary were adjusted to achieve the best fit between calculated and observed gravity anomalies along the profile.

The gravity model, presented in Fig. 14b, shows a good agreement between calculated and observed gravity values with a low RMS error of 1.6 mGal, which supports our interpretation of the Moho underneath line E. The good fit is achieved by assuming densities of 2180, 2400, 2600, 2990, and 3340 kg/m³ for syn-rift sediments, post-rift sediments, upper crust, lower crust, and mantle lithosphere, respectively. These density values are comparable with the density

model proposed by Lau et al. (2015) who assume slightly denser upper crust (2700 kg/m³) and mantle lithosphere (3350 kg/m³) along the OBWAVE line. The obtained mid-crust boundary (Fig. 14b) indicates strong upper and lower crustal thinning below the continental shelf and the eastern sub-basin. The upper crust is extremely thinned between 60 and 100 km and between 420 and 480 km, while the lower crust completely disappears beneath the edge of the continental shelf between 140 and 160 km and the eastern sub-basin between 370 and 420 km. Figure 16 shows that the mid-crustal boundary revealed by the gravity model is very consistent with the syn-rift structures inferred from the interpretation of seismic line E. The variations at the base of the upper crust somewhat coincide with the deep syn-rift normal faults, especially in the eastern Orphan sub-basin where the normal faults sole out at the Moho level and in the western Orphan sub-basin where the extensional faults die within the crust along a discontinuity which is roughly coincides with the predicted mid-crustal boundary (Fig. 16). However, the continental shelf at the western end of the section shows a sharp shallowing of the mid-crust boundary that is not related to any faulting (Fig. 16).

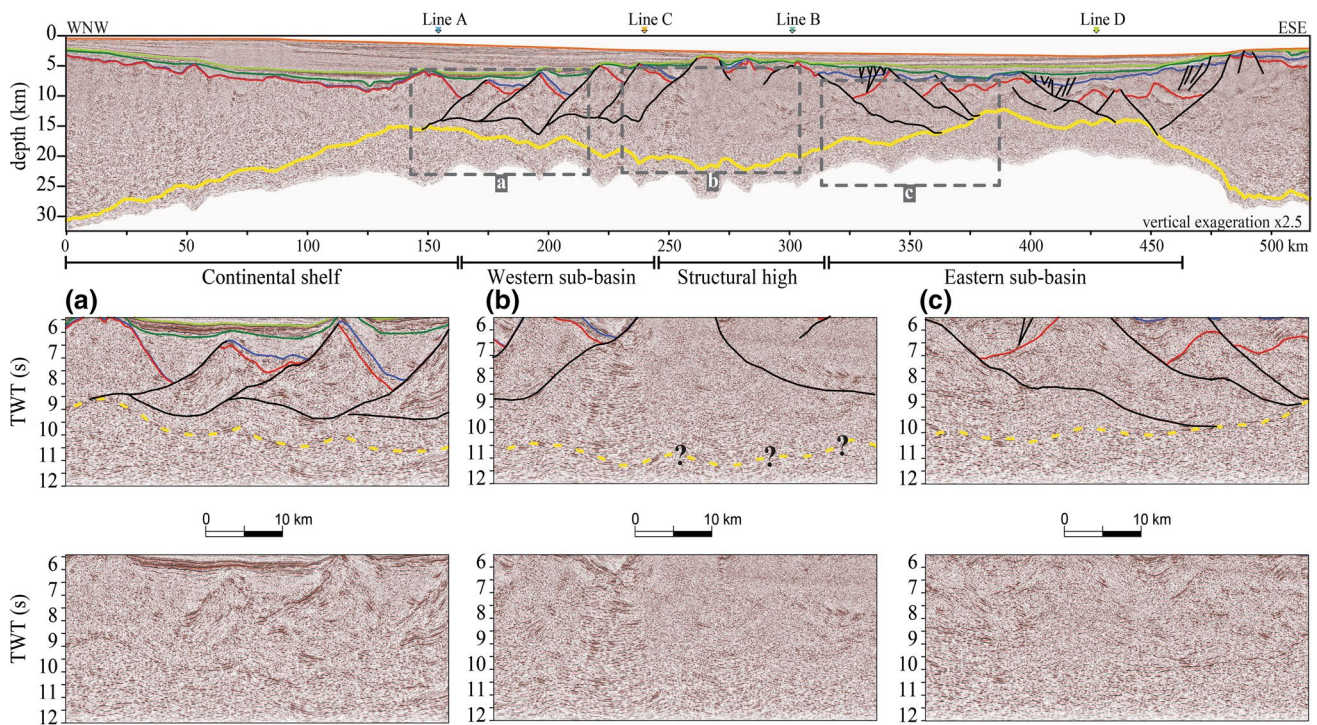
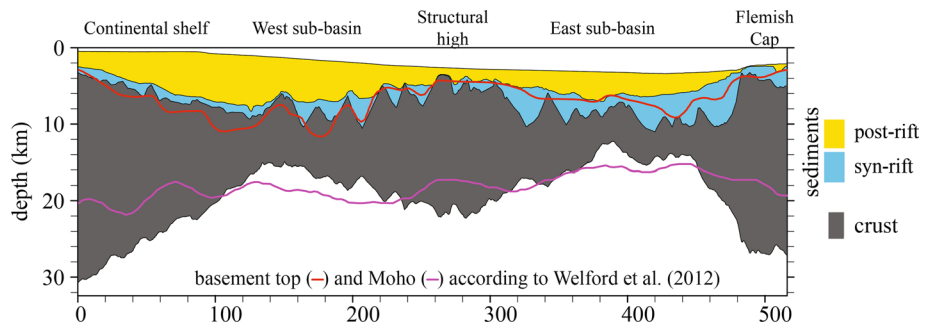


Fig. 12 Depth-converted seismic reflection line E showing the entire crustal architecture across the Orphan Basin. Profile location is shown in Fig. 2. The crustal domains from west to east are: the continental shelf, the western sub-basin, the structural high, and the east-

ern sub-basin. Interpretation of the Moho discontinuity is plotted with a *solid yellow line* and is shown in more detail in **a** to **c** (seismic data courtesy of TGS)

Fig. 13 Comparison between basement top and Moho from our seismic interpretation of Line E and from 3D gravity inversion after Welford et al. (2012)



Reconstruction of the tectono-stratigraphic evolution of the Orphan Basin

To reconstruct the tectonic evolution of the Orphan Basin and quantify the amount of crustal stretching during Mesozoic rifting, we restore crustal section E (Fig. 12) using the MOVE[®] software (<http://www.mve.com/>). The 2D restoration algorithm assumes two fundamental rules which are bed length conservation and bed area conservation. The former is based on the assumption that a given sedimentary bed keeps the same length before and after deformation. The latter rule assumes that deformation does not change the cross-sectional area of sedimentary

units. The kinematic restoration is based on the relationship between fault geometry and deformation patterns in the hanging walls of the normal faults, as documented along the seismic profile (Figs. 6, 10). Therefore, a simple shear model is used for most of the faults and the shear angle is defined based on the hanging-wall geometries (i.e. rollover structures, sedimentary growth, and flexural slip). Most of the normal faults show an antithetic shear angle ranging between 90 and 60°. During the restoration, decompaction is applied to the different lithostratigraphic successions using surface porosities and rates of decay with depth according to Sclater and Christie (1980). Decompaction requires palaeowater depth to be

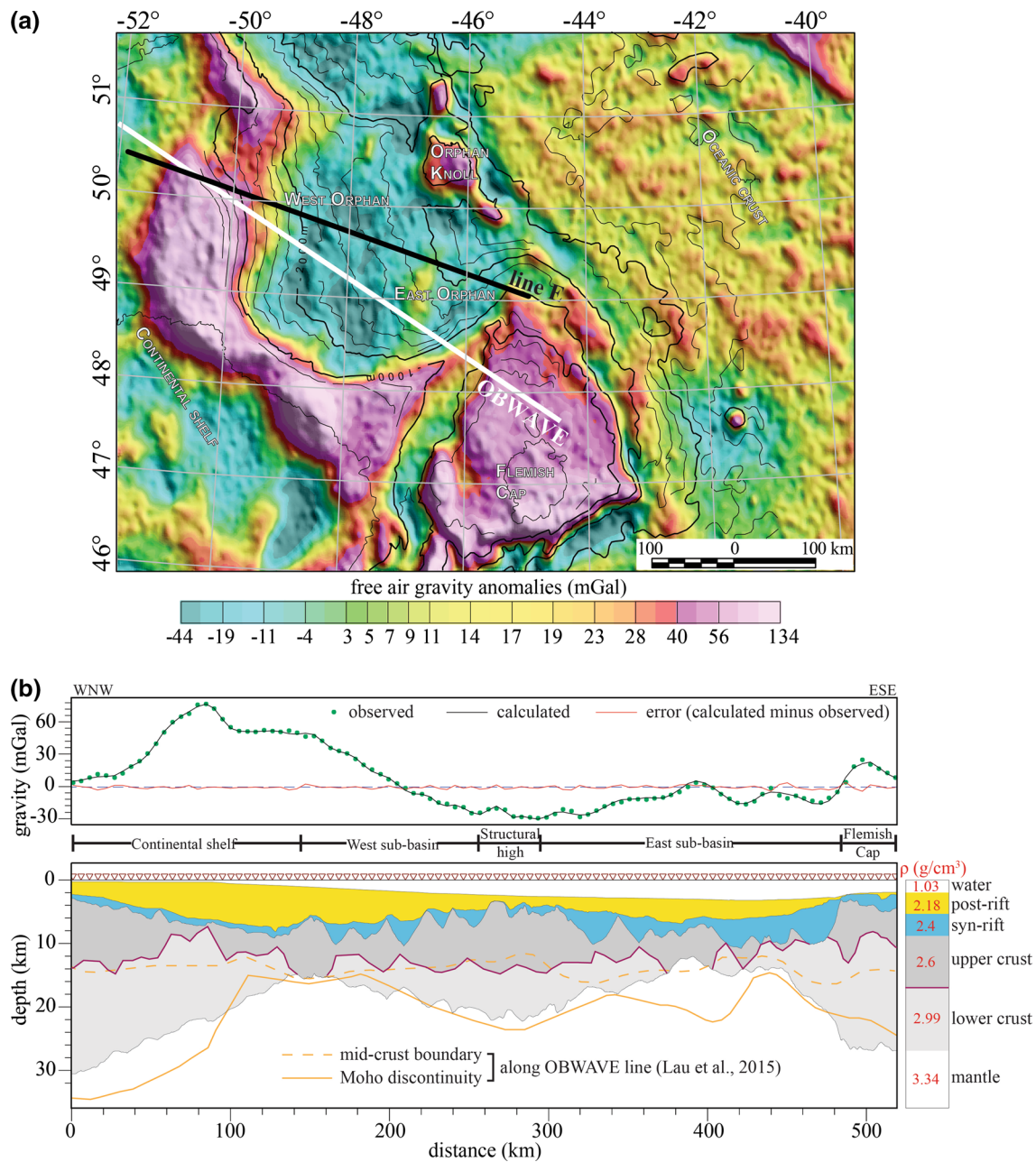


Fig. 14 **a** Free-air gravity anomalies over the Orphan Basin and surrounding areas with tracks of seismic line E in black and the OBWAVE line in white (Watremez et al. 2015; Lau et al. 2015). **b** Gravity model along line E: *upper panel* shows the observed and calculated gravity anomalies along line E; *lower panel* displays the

density model with the predicted mid-crust boundary (*solid purple line*). Calculated densities are indicated in red. For comparison, the mid-crust and Moho boundaries obtained along OBWAVE line are projected along our line E (Lau et al. 2015)

constrained along the profile. We assume that the basin remained at a very shallow position near sea level during the entire syn-rift period (i.e. from Jurassic to Late Cretaceous times). This is supported by the terrigenous nature of the Upper Jurassic and Lower Cretaceous sediments and by the emerged position of the basement highs (i.e. horsts and tilted block ridges) during that time and until the Late Cretaceous. We also assume that the basin started

to deepen in the Palaeocene and that the water depth increased linearly with time until it reached the present-day bathymetry. Local Airy isostasy is used to account for the isostatic response to sedimentary unloading during decompaction. We adopt average values for sediment (2300 kg/m^3), crust (2800 kg/m^3), and mantle (3340 kg/m^3) densities, which are inferred from the density model described above.

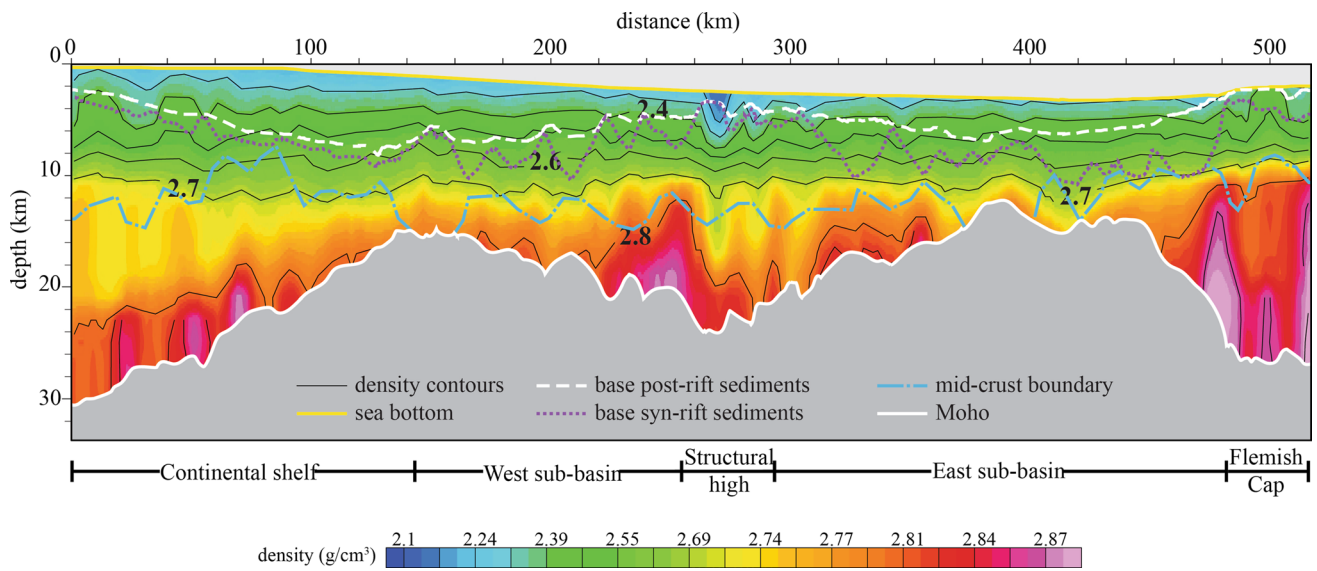


Fig. 15 Density grid along line E, calculated from interval velocities (Fig. 7) according to Gardner et al. (1974)

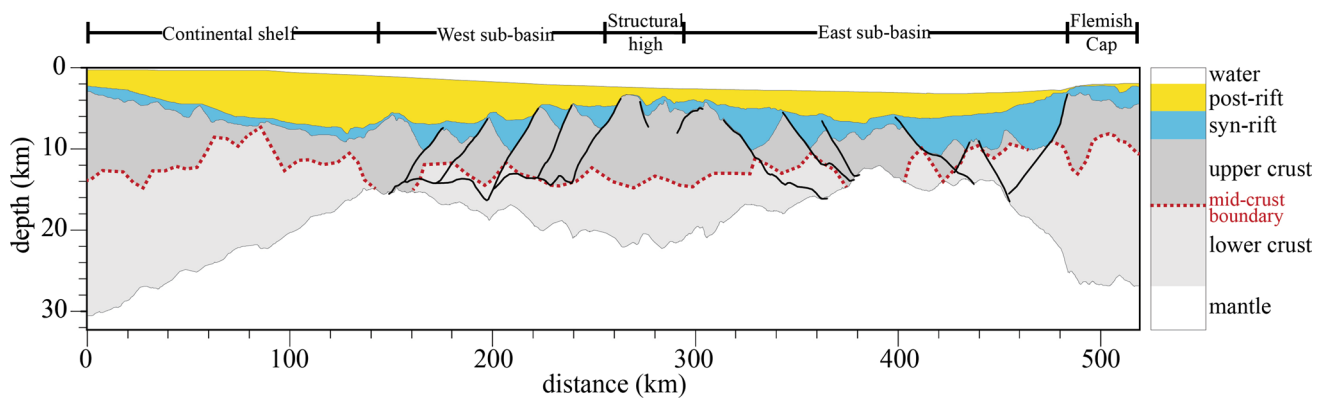


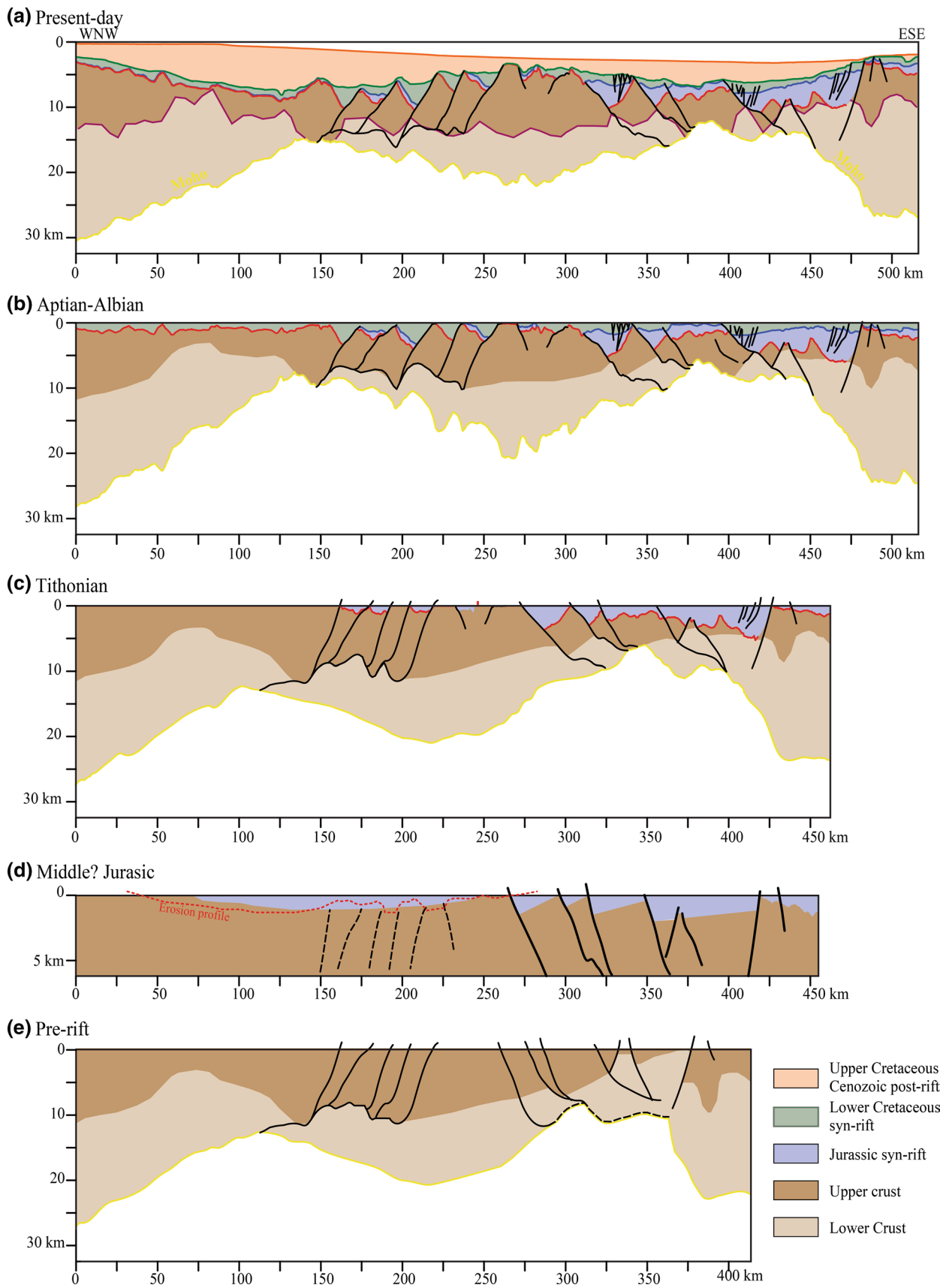
Fig. 16 Crustal section along line E showing correlation between the predicted mid-crust boundary and the syn-rift structures

Post-rift period

Restoring the post-rift strata consisted mainly of removing the water column and the Upper Cretaceous-Cenozoic successions (Fig. 17a, b), as most fault movements ended before the Late Cretaceous. The resulting decompaction affects primarily the western part of the profile (i.e. the continental shelf and the western sub-basin domains) where the thickest (up to 5 km) post-rift sediments are found. The structural architecture of the basin remained the same, except for minor changes in the angle of the normal faults in the western sub-basin domain which resulted in tilting of the faulted blocks by 2–4° further towards the east. The isostatic rebound resulted in a shallower Moho, especially beneath the sub-basins.

Syn-rift period

Syn-rift restoration was carried out in two steps. The first step consisted of removing the Lower Cretaceous succession, decompacting the Jurassic sediments, and restoring the normal faults to the end of Jurassic time (Fig. 17c). This step (Fig. 17c) substantially affected the western sub-basin domain where Early Cretaceous deformation is more pronounced. Extension is distributed along west-dipping normal faults, and tilting of the faulted blocks is compensated at the mid-crustal level. The obtained profile (Fig. 17c) shows a wide and continuous Jurassic basin in the east and isolated Jurassic troughs in the crustal high and western sub-basin domains. In contrast to the Jurassic sediments in the eastern sub-basin, which show syn-depositional tectonic structures (Fig. 10), the scattered Jurassic deposits to the west along



◀**Fig. 17** Kinematic and structural restoration of crustal line E, showing the evolution of the Orphan Basin. Each section is obtained by applying decompaction and fault restoration, starting from **a** the present-day profile, going through, **b** the Early Cretaceous, **c** the Late Jurassic, **d** the Middle Jurassic, and ending at **e** the pre-rift time. The restoration is accomplished using Move software (academic licence provided by Midland Valley Exploration)

the profile show no evidence of fault-controlled deposition (Fig. 11). Therefore, we assume that any (modest?) strata deposited in the western sub-basin early during the Jurassic syn-rift phase were eroded sometime before the initiation of the second rifting phase in the Early Cretaceous (Fig. 17d). The second syn-rift restoration step (Fig. 17e) involved removing the Jurassic succession and restoring the basement rocks. It mainly affected the eastern sub-basin, which was the locus of crustal stretching during the Jurassic.

Pre-rift crust

The restored pre-rift profile in Fig. 17e displays the crustal architecture prior to rifting, assuming that the Jurassic to Early Cretaceous extension was entirely accommodated by brittle deformation along the faults. It shows that the total extension is on the order of 110 km; 50 km of extension occurred during the Jurassic and was primarily accommodated by the east-dipping normal faults in the eastern sub-basin domain (Fig. 17c), while 60 km of extension is related to the Early Cretaceous rifting phase accommodated predominantly by the west-dipping normal faults (Fig. 17b). The restored profile (Fig. 17e) shows a 25- to 28-km-thick crust beneath the western part of the shelf, the western sub-basin and the crustal high domains, and a 10- to 12-km-thick crust beneath the eastern portion of the continental shelf and the eastern sub-basin domains. This is reflected in the topography of the restored mid-crust boundary (Fig. 17e), which displays two highs in the continental shelf domain and in the east sub-basin domain.

Similarly, seismic data and kinematic restoration of highly attenuated crustal domains found on the Iberian rifted margin (Manatschal et al. 2001; Manatschal 2004) indicate that the pre-faulting crustal thickness does not exceed 12 km. The authors argue that the pre-faulting stage does not correspond to a pre-rift stage, for which an equilibrated crust (i.e. 30 km thick) is assumed.

Discussion

Tectono-stratigraphic evolution of the Orphan Basin during rifting

Data presented in this work indicate that rifting in the Orphan Basin occurred in at least two phases. The initial Jurassic rifting phase affected mainly the eastern part of

the basin where continental extension is documented by east-dipping faults and thick Jurassic sediments, preserved in the hanging wall of the half-graben (Figs. 6, 10). Seismic reflections within the Jurassic succession show growth structures (Fig. 6), an indication that the normal faulting was coeval with, and controlled, sedimentary deposition. The Jurassic succession in the West Orphan Basin is substantially thinner and discontinuous with no evidence of syn-depositional tectonics (Figs. 6, 11). The major uncertainty in our seismic interpretation relates to the Jurassic deposits drilled only in the East Orphan Basin and for which there is no direct evidence in the west. However, the Deep-Sea Drilling Project (DSDP) Site 111, drilled on the Orphan Knoll, intersected coarse sandstone and shales at the base of the well that were determined to be Middle Jurassic (Bajocian) in age and above the Palaeozoic basement (Laughton et al. 1972). The compositions of these Middle Jurassic clastics indicate they were deposited in a coastal plain environment (Laughton et al. 1972), which we believe extended over most of the West Orphan Basin and may be part of the continental shelf.

The second rifting phase took place in the Early Cretaceous. During this phase, deformation spread towards the west of the Orphan Basin and resulted in half-graben bounded by west-dipping faults and filled by thick Lower Cretaceous deposits (Figs. 6, 11). In the east, some of the Jurassic east-dipping normal faults were reactivated and new sedimentary depocentres were developed (Fig. 6). Two-phase rifting in the Orphan Basin was already mentioned in previous work by Enachescu et al. (2005) who proposed an initial NW–SE extension in the Jurassic localized in the eastern part of the basin, and a late E–W extension which mainly affected the West Orphan Basin, but can also be documented in the east, during the Early Cretaceous. Seismic and well data indicate that rifting in the Orphan Basin was interrupted by two erosional events corresponding to the Tithonian and the Aptian–Albian truncation unconformities. The resulting angular unconformities between Jurassic and Lower Cretaceous strata (Tithonian unconformity), and Lower Cretaceous and Upper Cretaceous strata (Albian–Aptian unconformity) suggest that the basin was first uplifted then eroded. However, the duration of these uplift/erosion events remains difficult to constrain.

Late Cretaceous time marks the beginning of the post-rift stage as lithospheric break-up of the Newfoundland–Iberia/Europe rift occurred east of the Orphan Basin and the Grand Banks. Mantle lithosphere rocks were exhumed before the initiation of sea-floor spreading which occurred near the Aptian–Albian boundary (Tucholke et al. 2007). In the Orphan Basin, the Upper Cretaceous succession sealed most of the syn-rift structures but did not cover the structural highs (i.e. horsts and tilted block ridges), which remained above sea level at that time (Figs. 6, 10, 11). Some of the

west-dipping faults in the western part of the basin appear to have been reactivated during the Late Cretaceous (Figs. 6, 10, 11), probably in relation to the ongoing rifting to the north between Labrador and Greenland. It is only in the Palaeocene that the Orphan Basin evolves in a clearly post-rift setting, with a strong subsidence resulting in deposition of a thick Cenozoic succession over the rift structures.

Crustal extension and thinning in the Orphan Basin

The Moho and basement top in our interpretation of seismic line E (Fig. 12) indicate substantial variations in crustal thickness beneath the Orphan Basin. The crust is revealed to be significantly thin beneath the east and west sub-basins, and much thicker beneath the westernmost part of the continental shelf and the structural high separating the two sub-basins. The gravity modelling in this paper supports our interpretation of the seismic Moho as it shows that the observed free-air gravity anomalies can be explained by assuming a mid-crust boundary separating a low-density upper crust from a high-density lower crust (Fig. 14b). The obtained mid-crust boundary is consistent with the syn-rift structures imaged on the seismic data (Fig. 16). The syn-rift faults appear to be deeply rooted in the crust and sole out at the mid-crust boundary in West Orphan Basin and reach the Moho discontinuity in the East Orphan Basin where the crust is much thinner.

Our structural restoration (Fig. 17) shows that the observed brittle extension during rifting can explain only 60 % of the total thinning in the Orphan crust (i.e. in 2D along line E), assuming an initial pre-rift crustal thickness of 28 km—the maximum thickness observed beneath the continental shelf. The remaining crustal thinning is unlikely to be localized further offshore and should occur within the Orphan Basin because the crustal blocks surrounding the basin appear to be relatively undeformed—i.e. the Orphan Knoll and, especially, the Flemish Cap.

The discrepancy between recorded brittle extension and crustal thinning in the Orphan Basin is in accordance with the results of subsidence analysis. The latter shows that there is a large syn-rift subsidence deficit when we consider the amount of crustal thinning observed across the basin (Dafoe et al. 2015; Gouiza et al. 2015). According to Gouiza et al. (2015), the syn-rift succession should be at least 1.5–2.5 km thicker in the Orphan Basin. This may suggest the existence of, in addition to the preserved brittle extension, another extension phase that took place early during the rift process (Early Jurassic or even Late Triassic?) which is not easily recognizable on seismic data. Reston (2007, 2009) attributes the extension/thinning discrepancy to unrecognized polyphase faulting which is very difficult to identify in seismic data due to limitations in seismic resolution with depth and structural overprinting.

However, fault geometries, syn-rift stratigraphic architecture, and basement structures imaged in the examined seismic data do not provide solid evidence that polyphase rifting occurred in the Orphan Basin. Furthermore, Reston (2007) reckons that polyphase faulting is expected to occur in rifted margins where extension exceeds 100 % rather than in rift basins where crust is often less stretched (only 25 % of crustal extension in the Orphan Basin, along Line E). Alternatively, brittle extension in the Orphan Basin could be only partially preserved due to important crustal flexure, uplift, and erosion (Burov and Cloetingh 1997; Burov and Poliakov 2001). Well and seismic data presented above clearly indicate sub-aerial exposure and truncation of the syn-rift successions and tilted blocks (Enachescu et al. 2004; Dafoe et al. 2015). The existence of discontinuous pockets of Jurassic sediments in the West Orphan Basin might even be the remnants of a more extensive Jurassic or even Late Triassic (McAlpine 1990; Driscoll et al. 1995; Lau et al. 2006; Van Avendonk et al. 2009) syn-rift basin that have been eroded during the ensuing rift phase.

A hidden early rift phase, either unrecognized (i.e. polyphase faulting) or removed (i.e. uplifted and eroded), is not sufficient to explain the extension discrepancy in the Orphan Basin. Comparing lower and upper crustal thinning against whole crustal thinning (Fig. 18) shows that upper crustal thinning factors are higher in the continental shelf and the Flemish Cap (i.e. domains with the thickest crust; Fig. 12), while lower crustal thinning factors are higher in the eastern and western sub-basins (i.e. domains with the thinnest crust; Fig. 12). This is consistent with the findings of Lau et al. (2015) and Watremez et al. (2015) who constrained the Orphan Basin crust along the OBWAVE line (Fig. 14) using wide-angle seismic data and traveltimes tomography data, respectively. These observations are clear evidence of depth-dependent thinning within the crust and can indicate additional processes of ductile flow within the lower crust, mainly underneath domains of localized upper crustal brittle deformation, namely the East and West Orphan sub-basins.

Another source of uncertainty in quantifying the pre-rift crust is inheritance. The Mesozoic North Atlantic rift formed on remnants of the Palaeozoic Caledonian–Appalachian Orogeny, where the closure of the Iapetus Ocean led to continental collision, crustal and probably lithospheric thickening (imbrication of multiple terranes), crustal uplift, and erosion (Dewey and Kidd 1974; Williams 1984, 1995; McKerrow et al. 2000). The existence of four distinct crustal domains (namely the East Orphan sub-basin, the structural high, the West Orphan sub-basin, and the continental shelf), showing different deformation styles and migration of rifting, suggests that lateral heterogeneities—variations in thickness and/or rheology inherited from the pre-Mesozoic Caledonian–Appalachian Orogeny—may have played a crucial role in the tectonic evolution of the Orphan

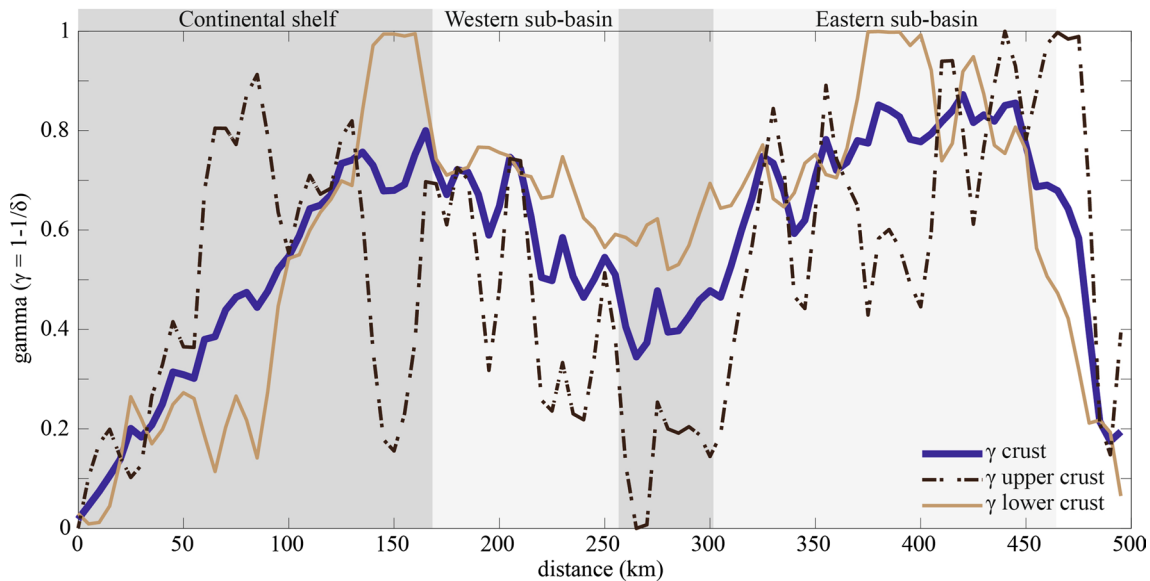


Fig. 18 Cross-plot showing variation of crustal, upper crustal, and lower crustal thinning factors ($\gamma = 1 - 1/\delta$, where δ = initial thickness divided by final thickness) along line E

Basin during, and following rifting (Smith and Mosley 1993; Vauchez et al. 1998; Huismans and Beaumont 2007; Gouiza et al. 2015; Chenin et al. 2015).

Conjugate Irish margin

Palaeoreconstructions of the North Atlantic Ocean to a time prior to lithospheric break-up and oceanic accretion (Chron M0; Fig. 1) show that the East and West Orphan sub-basins were juxtaposed against the Porcupine and the Rockall Basins, respectively, which are presently located on the conjugate Irish margin (Knott et al. 1993; Loudon et al. 2004). These three basins probably evolved as one large extensional system during the Mesozoic rifting (Lundin and Doré 2011; Lau et al. 2015) and should exhibit comparable stratigraphic, structural, and crustal syn-rift evolution.

Seismic data from the Porcupine and Rockall Basins indicate the presence of thick Late Palaeozoic to Cenozoic sedimentary successions (up to 10 km) overlying faulted blocks caused by extensive crustal stretching and suggest a multiphase Mesozoic syn-rift history (Mackenzie et al. 2002; Morewood et al. 2005; O'Reilly et al. 2006), similar to our observations from the Orphan Basin. The Porcupine Basin, where the syn-rift succession is well defined, shows three rift episodes of Permo-Triassic, Late Jurassic, and mid-Cretaceous age which were separated by periods of uplift and erosion (Morewood et al. 2005). The major episode of brittle extension is believed to be Jurassic, which is consistent with westward migration of the loci of rifting described in the Orphan Basin. Like in the Orphan Basin, the deep structures of the Porcupine and Rockall Basins are characterized by thick crust (25–30 km) beneath

the basin-bounding highs and highly thinned crust below the basins (2–10 km) (Morewood et al. 2005; O'Reilly et al. 2006). The Moho beneath the two basins shows a very pronounced asymmetry that is less evident in the Orphan Basin, but we do observe a lateral offset between areas of main upper crustal faulting and areas of extreme lower crustal thinning, especially in the western sub-basin (Fig. 12). The major difference between the two conjugate margins is revealed by the various velocity models which show strong evidence of low-velocity serpentinized mantle beneath the highly thinned crust in the Porcupine and Rockall Basins, but not in the Orphan Basin (Chian et al. 2001; Morewood et al. 2005; O'Reilly et al. 2006; Watremez et al. 2015; Lau et al. 2015).

Conclusions

The Orphan Basin, located offshore of the Newfoundland rifted margin, is a broad deepwater rift basin, characterized by thick Mesozoic to Cenozoic sedimentary successions which overlie a highly thinned continental crust.

The deep seismic reflection data used in this work clearly demonstrate the existence of strong brittle deformation coupled with a high degree of crustal thinning. Sedimentary successions, preserved in the Orphan Basin, suggests a two-phase rifting during the Jurassic and the Early Cretaceous, respectively, separated by periods of uplift and erosion. Upper crustal extension initiated in the east sub-basin in the Jurassic and spread to the west sub-basin in the Early Cretaceous. The latter experienced a late phase of deformation that reactivated the syn-rift structures and

that was likely related to the contemporaneous rifting to the north in the Labrador Sea.

However, the interpreted structural and crustal architectures in the Orphan Basin suggest that the observed brittle extension does not fully match the quantified crustal thinning. An Early Jurassic, or even Late Triassic, brittle rift phase and localized thinning by ductile flow in the lower crust are proposed as additional processes that could have contributed to continental deformation in the basin.

Acknowledgments This work is a contribution to the project of Plate Reconstruction of the North Atlantic between Ireland and Canada, part of the work programme of the North Atlantic Petroleum Systems Assessment initiated by the Petroleum Infrastructure Programme in Ireland and Memorial University of Newfoundland. The research is funded by Nalcor Energy, Husky Energy and the Natural Sciences and Engineering Research Council of Canada. Seismic data are shown courtesy of TGS. Midland Valley Exploration provided the academic licence for the Move software, and Schlumberger provided the licence for the Petrel software. We are grateful to Garry Karner, Harm Van Avendonk, Tiago M. Alves, and Tim Minshull for reviewing earlier versions of the manuscript and for their constructive comments.

Open Access This article is distributed under the terms of the Creative Commons Attribution 4.0 International License (<http://creativecommons.org/licenses/by/4.0/>), which permits unrestricted use, distribution, and reproduction in any medium, provided you give appropriate credit to the original author(s) and the source, provide a link to the Creative Commons license, and indicate if changes were made.

References

- Alves TM, Gawthorpe RL, Hunt DW, Monteiro JH (2003) Cenozoic tectono-sedimentary evolution of the western Iberian margin. *Mar Geol* 195:75–108. doi:10.1016/S0025-3227(02)00683-7
- Alves TM, Moita C, Sandnes F et al (2006) MesozoicdashCenozoic evolution of North Atlantic continental-slope basins: the Peniche basin, western Iberian margin. *AAPG Bull* 90:31–60. doi:10.1306/08110504138
- Alves TM, Moita C, Cunha T et al (2009) Diachronous evolution of Late Jurassic-Cretaceous continental rifting in the northeast Atlantic (west Iberian margin). *Tectonics* 28:TC4003. doi:10.1029/2008TC002337
- Bassi G, Keen CE, Potter P (1993) Contrasting styles of rifting: models and examples from the Eastern Canadian Margin. *Tectonics* 12:639–655. doi:10.1029/93TC00197
- Burov E, Cloetingh S (1997) Erosion and rift dynamics: new thermomechanical aspects of post-rift evolution of extensional basins. *Earth Planet Sci Lett* 150:7–26. doi:10.1016/S0012-821X(97)00069-1
- Burov E, Poliakov A (2001) Erosion and rheology controls on synrift and postrift evolution: verifying old and new ideas using a fully coupled numerical model. *J Geophys Res* 106:16461–16481. doi:10.1029/2001JB000433
- Chalmers JA, Pulvertaft TCR, Marcussen C, Pedersen AK (1999) New insight into the structure of the Nuussuaq Basin, central West Greenland. *Mar Pet Geol* 16(197–211):213–224. doi:10.1016/S0264-8172(98)00077-4
- Chenin P, Manatschal G, Lavier LL, Erratt D (2015) Assessing the impact of orogenic inheritance on the architecture, timing and magmatic budget of the North Atlantic rift system: a mapping approach. *J Geol Soc* 172:711–720. doi:10.1144/jgs2014-139
- Chian D, Loudon KE, Reid I (1995) Crustal structure of the Labrador Sea conjugate margin and implications for the formation of nonvolcanic continental margins. *J Geophys Res Solid Earth* 100:24239–24253. doi:10.1029/95JB02162
- Chian D, Reid ID, Jackson HR (2001) Crustal structure beneath Orphan Basin and implications for nonvolcanic continental rifting. *J Geophys Res Solid Earth* 106:10923–10940. doi:10.1029/2000JB900422
- Dafoe LT, Keen CE, Dickie K, Williams GL (2015) Regional stratigraphy and subsidence of Orphan Basin near the time of breakup and implications for rifting processes. *Basin Res*. doi:10.1111/bre.12147
- Dewey JF, Kidd WSF (1974) Continental collisions in the Appalachian–Caledonian orogenic belt: variations related to complete and incomplete suturing. *Geology* 2:543–546. doi:10.1130/0091-7613(1974)2<543:CCITAO>2.0.CO;2
- Dickie K, Keen CE, Williams GL, Dehler SA (2011) Tectonostratigraphic evolution of the Labrador margin, Atlantic Canada. *Mar Pet Geol* 28:1663–1675. doi:10.1016/j.marpetgeo.2011.05.009
- Dix CH (1955) Seismic velocities from surface measurements. *Geophysics* 20:68–86. doi:10.1190/1.1438126
- Driscoll NW, Hogg JR, Christie-Blick N, Karner GD (1995) Extensional tectonics in the Jeanne d'Arc Basin, offshore Newfoundland: implications for the timing of break-up between Grand Banks and Iberia. *Geol Soc Lond Spec Publ* 90:1–28. doi:10.1144/GSL.SP.1995.090.01.01
- Enachescu ME (2006) Structural setting and petroleum potential of the Orphan Basin, offshore Newfoundland and Labrador. *Recorder* 31:5–13
- Enachescu ME, Kearsley S, Hogg J et al (2004) Orphan Basin, offshore Newfoundland, Canada: structural and tectonic framework, petroleum systems and exploration potential. In: Society of exploration geophysicists (SEG) 74th annual meeting and exposition, expanded abstracts, pp 382–385
- Enachescu ME, Kearsley S, Hardy V et al (2005) Evolution and petroleum potential of Orphan Basin, offshore Newfoundland, and its relation to the movement and rotation of Flemish Cap based on plate kinematics of the North Atlantic. In: 25th annual Gulf Coast section SEPM Foundation, Bob F. Perkins research conference, symposium on petroleum systems of divergent continental margin basins. Society for Sedimentary Geology, Gulf Coast Section, Dallas, TX, pp 7–8
- Funck T, Hopper JR, Larsen HC et al (2003) Crustal structure of the ocean–continent transition at Flemish Cap: seismic refraction results. *J Geophys Res* 108(20):2003. doi:10.1029/2003JB002434
- Gacal-Isler B (2009) Mesozoic tectonic and stratigraphic evolution of the Orphan Basin, with special emphasis on regional correlations with Flemish Pass and northern Jeanne d'Arc Basins, Grand Banks of Newfoundland. Master Thesis, Memorial University of Newfoundland
- Gardner GHF, Gardner LW, Gregory AR (1974) Formation velocity and density—the Diagnostic basics for stratigraphic traps. *Geophysics* 39:770–780. doi:10.1190/1.1440465
- Gouiza M, Hall J, Bertotti G (2015) Rifting and pre-rift lithosphere variability in the Orphan Basin, Newfoundland margin, Eastern Canada. *Basin Res* 27:367–386. doi:10.1111/bre.12078
- Grant AC, McAlpine KD (1990) The continental margin around Newfoundland. In: Keen MJ, Williams GL (eds) *Geology of the continental margin of Eastern Canada*, Geology of Canada. Geological Survey of Canada, Ottawa, pp 241–292
- Huisman RS, Beaumont C (2007) Roles of lithospheric strain softening and heterogeneity in determining the geometry of rifts and continental margins. *Geol Soc Lond Spec Publ* 282:111–138. doi:10.1144/SP282.6

- Knott SD, Burchell MT, Jolley EJ, Fraser AJ (1993) Mesozoic to Cenozoic plate reconstructions of the North Atlantic and hydrocarbon plays of the Atlantic margins. *Geol Soc Lond Pet Geol Conf Ser* 4:953–974. doi:[10.1144/0040953](https://doi.org/10.1144/0040953)
- Lau KWH, Loudon KE, Funck T et al (2006) Crustal structure across the Grand Banks-Newfoundland Basin Continental Margin—I. Results from a seismic refraction profile. *Geophys J Int* 167:127–156
- Lau KWH, Watremez L, Loudon KE, Nedimović MR (2015) Structure of thinned continental crust across the Orphan Basin from a dense wide-angle seismic profile and gravity data. *Geophys J Int* 202:1969–1992. doi:[10.1093/gji/ggv261](https://doi.org/10.1093/gji/ggv261)
- Laughton AS, Berggren WA et al (1972) Initial reports of the Deep Sea Drilling Project, 12. U.S. Government Printing Office, Washington, DC
- Loudon KE, Tucholke BE, Oakey GN (2004) Regional anomalies of sediment thickness, basement depth and isostatic crustal thickness in the North Atlantic Ocean. *Earth Planet Sci Lett* 224:193–211. doi:[10.1016/j.epsl.2004.05.002](https://doi.org/10.1016/j.epsl.2004.05.002)
- Lundin ER, Doré AG (2011) Hyperextension, serpentinization, and weakening: a new paradigm for rifted margin compressional deformation. *Geology* 39:347–350. doi:[10.1130/G31499.1](https://doi.org/10.1130/G31499.1)
- Mackenzie GD, Shannon PM, Jacob AWB et al (2002) The velocity structure of the sediments in the southern Rockall Basin: results from new wide-angle seismic modelling. *Mar Pet Geol* 19:989–1003. doi:[10.1016/S0264-8172\(02\)00133-2](https://doi.org/10.1016/S0264-8172(02)00133-2)
- Manatschal G (2004) New models for evolution of magma-poor rifted margins based on a review of data and concepts from West Iberia and the Alps. *Int J Earth Sci*. doi:[10.1007/s00531-004-0394-7](https://doi.org/10.1007/s00531-004-0394-7)
- Manatschal G, Froitzheim N, Rubenach M, Turrin BD (2001) The role of detachment faulting in the formation of an ocean-continent transition: insights from the Iberia Abyssal Plain. *Geol Soc Lond Spec Publ* 187:405–428. doi:[10.1144/GSL.SP.2001.187.01.20](https://doi.org/10.1144/GSL.SP.2001.187.01.20)
- McAlpine KD (1990) Mesozoic stratigraphy, sedimentary evolution, and petroleum potential of the Jeanne d’Arc Basin, Grand Banks of Newfoundland. Geological Survey of Canada, Ottawa
- McKerrow WS, Niocailh CM, Dewey JF (2000) The Caledonian Orogeny redefined. *J Geol Soc* 157:1149–1154. doi:[10.1144/jgs.157.6.1149](https://doi.org/10.1144/jgs.157.6.1149)
- Morewood NC, Mackenzie GD, Shannon PM et al (2005) The crustal structure and regional development of the Irish Atlantic margin region. *Geol Soc Lond Pet Geol Conf Ser* 6:1023–1033. doi:[10.1144/0061023](https://doi.org/10.1144/0061023)
- Murphy NJ, Ainsworth NR (1991) Stratigraphy of the Triassic, Lower Jurassic and Middle Jurassic (Aalenian) from the Fastnet Basin, offshore south-west Ireland. *Mar Pet Geol* 8:417–429. doi:[10.1016/0264-8172\(91\)90064-8](https://doi.org/10.1016/0264-8172(91)90064-8)
- O’Reilly BM, Hauser F, Ravaut C et al (2006) Crustal thinning, mantle exhumation and serpentinization in the Porcupine Basin, offshore Ireland: evidence from wide-angle seismic data. *J Geol Soc* 163:775–787. doi:[10.1144/0016-76492005-079](https://doi.org/10.1144/0016-76492005-079)
- Pe-Piper G, Meredyk S, Zhang Y et al (2013) Petrology and tectonic significance of seamounts within transitional crust east of Orphan Knoll, offshore eastern Canada. *Geo-Mar Lett* 33:433–447. doi:[10.1007/s00367-013-0342-2](https://doi.org/10.1007/s00367-013-0342-2)
- Reston T (2007) Extension discrepancy of North Atlantic nonvolcanic rifted margins: depth-dependent stretching or unrecognized faulting? *Geology* 35:367–370
- Reston TJ (2009) The extension discrepancy and syn-rift subsidence deficit at rifted margins. *Pet Geosci* 15:217–237. doi:[10.1144/1354-079309-845](https://doi.org/10.1144/1354-079309-845)
- Roberts DG, Bally AW (2012) Regional geology and tectonics: Phanerozoic rift systems and sedimentary basins: Phanerozoic rift systems and sedimentary basins. Elsevier, Amsterdam
- Sandwell DT, Smith WHF (2009) Global marine gravity from retracked Geosat and ERS-1 altimetry: ridge segmentation versus spreading rate. *J Geophys Res Solid Earth* 114:B01411. doi:[10.1029/2008JB006008](https://doi.org/10.1029/2008JB006008)
- Sclater JG, Christie PAF (1980) Continental stretching: an explanation of the post-mid-Cretaceous subsidence of the central North Sea basin. *J Geophys Res* 85:3711–3739
- Shannon PM, Corcoran DV, Haughton PDW (2001) The petroleum exploration of Ireland’s offshore basins: introduction. *Geol Soc Lond Spec Publ* 188:1–8. doi:[10.1144/GSL.SP.2001.188.01.01](https://doi.org/10.1144/GSL.SP.2001.188.01.01)
- Smith M, Mosley P (1993) Crustal heterogeneity and basement influence on the development of the Kenya Rift, East Africa. *Tectonics* 12:591–606. doi:[10.1029/92TC01710](https://doi.org/10.1029/92TC01710)
- Soares DM, Alves TM, Terrinha P (2012) The breakup sequence and associated lithospheric breakup surface: their significance in the context of rifted continental margins (West Iberia and Newfoundland margins, North Atlantic). *Earth Planet Sci Lett* 355–356:311–326. doi:[10.1016/j.epsl.2012.08.036](https://doi.org/10.1016/j.epsl.2012.08.036)
- Tankard AJ, Welsink HJ (1989) Mesozoic extension and styles of basin formation in Atlantic Canada. *Ext Tecton Stratigr N Atl Margins AAPG Mem* 46:175–195
- Tucholke BE, Sibuet J-C (2012) Problematic plate reconstruction. *Nat Geosci* 5:676–677. doi:[10.1038/ngeo1596](https://doi.org/10.1038/ngeo1596)
- Tucholke BE, Sawyer DS, Sibuet J-C (2007) Breakup of the Newfoundland-Iberia rift. *Geol Soc Lond Spec Publ* 282:9–46. doi:[10.1144/SP282.2](https://doi.org/10.1144/SP282.2)
- Van Avendonk HJA, Lavier LL, Shillington DJ, Manatschal G (2009) Extension of continental crust at the margin of the eastern Grand Banks, Newfoundland. *Tectonophysics* 468:131–148. doi:[10.1016/j.tecto.2008.05.030](https://doi.org/10.1016/j.tecto.2008.05.030)
- Vauchez A, Tommasi A, Barruol G (1998) Rheological heterogeneity, mechanical anisotropy and deformation of the continental lithosphere. *Tectonophysics* 296:61–86. doi:[10.1016/S0040-1951\(98\)00137-1](https://doi.org/10.1016/S0040-1951(98)00137-1)
- Vogt U, Makris J, O’Reilly BM et al (1998) The Hatton Basin and continental margin: crustal structure from wide-angle seismic and gravity data. *J Geophys Res Solid Earth* 103:12545–12566. doi:[10.1029/98JB00604](https://doi.org/10.1029/98JB00604)
- Watremez L, Lau KWH, Nedimović MR, Loudon KE (2015) Travel-time tomography of a dense wide-angle profile across Orphan Basin. *Geophysics* 80:B69–B82. doi:[10.1190/geo2014-0377.1](https://doi.org/10.1190/geo2014-0377.1)
- Welford JK, Hall J (2007) Crustal structure of the Newfoundland rifted continental margin from constrained 3-D gravity inversion. *Geophys J Int* 171:890–908
- Welford JK, Hall J, Sibuet J-C, Srivastava SP (2010) Structure across the northeastern margin of Flemish Cap, offshore Newfoundland from Erable multichannel seismic reflection profiles: evidence for a transtensional rifting environment. *Geophys J Int* 183:572–586. doi:[10.1111/j.1365-246X.2010.04779.x](https://doi.org/10.1111/j.1365-246X.2010.04779.x)
- Welford JK, Shannon PM, O’Reilly BM, Hall J (2012) Comparison of lithosphere structure across the Orphan Basin-Flemish Cap and Irish Atlantic conjugate continental margins from constrained 3D gravity inversions. *J Geol Soc* 169:405–420. doi:[10.1144/0016-76492011-114](https://doi.org/10.1144/0016-76492011-114)
- Welsink HJ, Srivastava SP, Tankard AJ (1989) Basin architecture of the Newfoundland continental margin and its relationship to ocean crust fabric during extension. *Ext Tecton Stratigr N Atl Margins AAPG Mem* 46:197–213
- Williams H (1984) Miogeoclines and suspect terranes of the Caledonian–Appalachian Orogen: tectonic patterns in the North Atlantic region. *Can J Earth Sci* 21:887–901. doi:[10.1139/e84-095](https://doi.org/10.1139/e84-095)
- Williams H (1995) Geology of the Appalachian–Caledonian Orogen in Canada and Greenland. Geological Survey of Canada, Ottawa
- Yang Y-T (2012) Tectonostratigraphic evolution of the northern Porcupine Basin, Irish Atlantic margin, during the Late Jurassic–Early Cretaceous, implication for a regional compressional event. *Mar Pet Geol* 36:140–153. doi:[10.1016/j.marpetgeo.2012.05.003](https://doi.org/10.1016/j.marpetgeo.2012.05.003)